CHALMERS

Improved QCM-D Signal Sensitivity Using Mesoporous Silica

Master of Science Thesis [in the Master Degree Programme, Advanced Engineering Materials]

AKBAR AHMADI

Department of Chemical and Biological Engineering
Division of Applied Surface Chemistry
CHALMERS UNIVERSITY OF TECHNOLOGY
Göteborg, Sweden, 2011

THESIS FOR THE DEGREE OF MASTER OF SCIENCE

Improved QCM-D Signal Sensitivity Using Mesoporous Silica

AKBAR AHMADI

CHALMERS

Supervised by Maria Claesson & Martin Andersson
Examined by Prof. Krister Holmberg

Department of Chemical and Biological Engineering
CHALMERS UNIVERSITY OF TECHNOLOGY

Göteborg, Sweden, 2011

Improved QCM-D Signal Sensitivity Using Mesoporous Silica

Department of Chemical and Biological Engineering
CHALMERS UNIVERSITY OF TECHNOLOGY
SE-412 96 Göteborg
Sweden
Telephone +46 (0)31-772 2750

To my little angel, ***Anahita***

Improved QCM-D Signal Sensitivity Using Mesoporous Silica

AKBAR AHMADI
Applied Surface Chemistry
Department of Chemical and Biological Engineering
Chalmers University of Technology

Abstract

Quartz crystal microbalance with dissipation monitoring (QCM-D) is a mass sensing technique that is used to study the adsorption of different species and their interaction with different types of surfaces in real time. The technique is commonly used since it is simple, cost effective and provides high-resolution mass sensing.

This project aimed at investigating the possibility of improving the sensitivity of the QCM-D signal by adsorbing four different generations (G0, G1, G2 and G3) of polyamidoamine (PAMAM) dendrimers on mesoporous silica having varying pore size and non-porous silica coated QCM-D sensor crystals. Furthermore, the adsorption of different ions and small molecules on the various surfaces was investigated.

The obtained results showed that mesoporous silica improved the sensitivity of the QCM-D signal. This was observed as a large shift in frequency upon adsorption of dendrimers on mesoporous silica compared to on non-porous silica. The sensitivity was improved on all mesoporous silica surfaces regardless of pore size; however, no correlation between the pore size and the size of the adsorbed dendrimers could be observed. The shift in dissipation was low and similar on all surfaces regardless of the size of the adsorbed dendrimers, which indicated that the formed dendrimer layer can be compared whit a rigid film. Additionally, no significant shift in frequency or dissipation was observed for the adsorption of ions or small molecules on the investigated surfaces.

To conclude, mesoporous silica is considered to be a promising material to use to enhance the signal sensitivity of the QCM-D. The material is advantageous to use since the properties, such as pore size, pore geometry and surface chemistry easily can be tailor-made depending on the application.

Keywords: QCM-D, mesoporous silica, dendrimers, sensitivity

Table of contents

1. Introduction

During the last decades, research and development (R&D) on sensors has grown exponentially. A sensor provides information on the physical, chemical and biological environment. A huge demand for the sensors origins by legislation for environmental monitoring, e.g. monitoring toxic gases and vapors in the workplace or contaminants in natural waters by industrial sewage and agricultural runoff [1].

One of the most important areas in the field of chemical sensing is mass sensing. The transduction principle in a mass sensor is the detection of the mass change through the changes in behavior of some oscillator. Piezoelectric crystals have been utilized as microbalances because of their small size, high sensitivity, and stability. The effect of added mass on the crystal frequency has been known since the early days of radio when pencil marks on the controlling quartz crystal was utilized to adjust the frequency [2]. Sauerbrey was the first who investigated the suitability of quartz crystal for determining mass [3].

Mass sensors were synonymous with the quartz crystal microbalance (QCM), at the beginning of their development. Later on, other oscillators, such as the Surface Acoustic Wave (SAW) devices, vibrating beams, and cantilevers, were added which may employ different oscillatory modes and are made from other materials and sometimes from non-piezoelectric materials [4].

QCM is commonly used to study changes in mass, since it is a simple, cost effective, high-resolution mass sensing method. In most applications, only changes of resonant frequency (Δf) of the adsorbed layers on the sensor surface is monitored. A variation of the QCM has been developed, which also allows for the monitoring of dissipation (D) of the sensor at the same time. The D-factor is related to the viscoelastic properties of the adsorbed layer. The new QCM modification, called QCM with dissipation monitoring or QCM-D, has increased the analytical range of the instrument in different fields like electrochemistry and biology [5, 6]. QCM-D has furthermore been employed to study the adsorption behavior of different species and their interaction with different types of surfaces in real time.

This project aimed at investigating the adsorption behavior of four different generations of polyamidoamine (PAMAM) dendrimers on mesoporous and non-porous silica using QCM-D, to study the possibility of increasing the mass sensitivity of QCM-D technique. The experiments were performed by depositing mesoporous silica thin film having varying pore size on silica coated QCM-D crystals and then study the adsorption behavior of PAMAM dendrimers on the various surfaces.

1.1. QCM-D

The quartz crystal microbalance with dissipation monitoring (QCM-D) technique is a nanogram sensitive technique to study the adsorption behavior of species on solid surfaces. The technique measures mass changes utilizing acoustic waves that are generated by oscillation of a piezoelectric quartz crystal. By applying an electric field to quartz, it starts to oscillate (expansion and contraction of the crystal lattice) at a certain frequency, which is related to the crystal mass [7]. The oscillation frequency changes with increasing mass of the crystal due to the adsorption of species on its surface. If the adsorbed mass is a) small compared to the mass of the crystal, and is adsorbed b) rigidly and c) evenly distributed over the active area of the crystal, the mass of the adsorbed species, Δm, can be related to the frequency change, Δf, by the Sauerbrey equation (1) [8]:

$$\Delta m = \frac{C}{n} \Delta f \qquad (1)$$

where $C = t_q \rho_q / f_0$ is the mass sensitivity constant and equals -17.7 ng.Hz^{-1}.cm^{-2} for a 5 MHz crystal, t_q and ρ_q are the thickness and density of the quartz crystal, f_0 is the fundamental resonant frequency of the crystal in air, and n is the overtone number (=1, 3, 5, …). When one of the above mentioned conditions does not meet, equation 1 is not valid.

The QCM was in the beginning only used as a gas-phase mass detector. In the beginning of 1980´s it was realized that a quartz crystal completely immersed in a liquid also can oscillate [9]. However, the amplitude of the oscillation of the crystal decreases severely in contact with liquid compared to in vacuum or gas, which is because liquids have much higher viscosities. Furthermore, the induced shear waves can be damped more rapidly by exposure to molecules dispersed in water i.e. larger energy dissipation. The adsorbed species on the surface change the frequency as well as the energy dissipation rate in response to changes in mass and viscoelastic properties, respectively. So, by measuring dissipation and frequency changes simultaneously, the adsorption process can be studied in terms of mass and viscoelastic properties. Kanazawa and coworkers, the pioneers in liquid phase QCM measurements, showed that the viscoselastic resonance frequency change (Δf_v) of a QCM in a liquid can be expressed by the relation described in equation (2) [10]:

$$\Delta f_v = - f_0^{3/2} \left(\frac{\eta_l \rho_l}{\pi \mu_q \rho_q} \right)^{1/2} \qquad (2)$$

where η_l and ρ_l are the viscosity and density of the liquid medium, respectively, and μ_q is the elastic modulus of the quartz crystal. The dissipation factor (D), i.e. the

energy loss of the crystal due to the coupling of its motion to the surrounding liquid, can be calculated according to equation (3):

$$D = \frac{4}{t_q \rho_q} \left(\frac{\eta_l \rho_l}{2\omega} \right)^{1/2} \quad (3)$$

where ω is the angular frequency [10].

A QCM sensor is a thickness shear mode (TSM) acoustic wave resonator consists of an AT-cut thin quartz disk sandwiched between two metal electrodes (typically gold). The AT-cut disk is a cut from a quartz mineral at a 35° 10′ orientation to its optical axis and has high temperature stability and pure shear motion in the electric field (Figure 1). By applying an alternating electric field a shear (tangential) deformation is produced in the quartz crystal, which results in that both surfaces move in parallel but opposite directions (motion antinodes) [11, 12].

1.2. Mesoporous Silica

Porous materials have attracted extensive attention due to their great potentials in versatile applications, e.g. adsorption technology, molecular separation, catalysis, biomedicine, electronics, gas sensors, etc. These materials often have high surface areas and large pore volumes. International Union of Pure and Applied Chemistry (IUPAC) has classified pores into three categories according to their sizes [13]:

- pores with widths exceeding about 50 nm (500 Å) are called macropores
- pores with widths not exceeding about 2.0 nm (20 Å) are called micropores
- pores of intermediate size (2-50 nm) are called mesopores

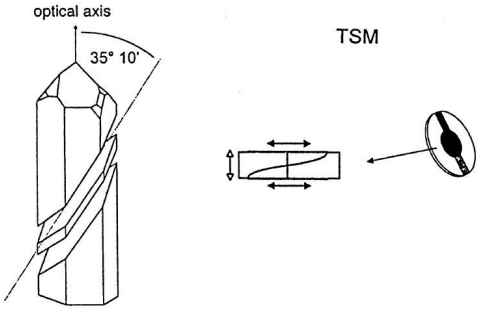

Figure 1: *AT-cut of a quartz crystal from which the metal coated QCM quartz crystals are produced. Furthermore an end of a crystal is viewed illustrating the thickness shear mode (TSM) of oscillation [11]*

Mesoporous materials have been known for a couple of decades. For instance, pillared clays with pores in the meso range have been extensively investigated since the 1980s. However, some disadvantages of these materials exists when used as catalysts and adsorption media due to their disordered arrangement of pores, wide pore size distribution and not fully opened pores [14].

In the early 1990s, the synthesis of mesostructued silicates was reported separately by Japanese scientists and Mobil Oil scientists [15, 16]. This new family of porous materials designated as M41S has an ordered array of uniform and controllable mesopores and was formed using a "liquid crystalline template" (LCT). The mechanism behind the formation of mesostructured silicates is to use templating molecules, such as long chain quaternary ammonium cationic surfactants, to organize as a liquid crystal onto which precursor molecules are self-assembled (Fig. 2). The inorganic precursors create walls between the surfactant cylinders. This is followed by removal of the liquid template as well as formation of stable mesostructure by subsequently thermal processing [16, 17]. Before these reports, a US patent had been filed in 1971 by Chiola et al. [18] in which the obtained material was found to be similar to MCM-41 (Mobil Composition of Matter No 41) in terms of the synthesis procedure and structure [19]. The 2D-hexagonal mesostructured MCM-41 is the best known and most widely studied material of M41S family. Other members of this family, MCM-48 and MCM-50, were discovered several months after MCM-41 during detailed studies to relate the surfactant concentration and the silica reagent (Fig. 3). These two materials have cubic and lamellar mesostructures, respectively [20]. M41S family of materials has uniform and controllable pore size and extremely high surface area. In 1995, researcher focused on developing mesoporous molecular sieves like hexagonal mesoporous silica (HMS) and Michigan State University (MSU) family of materials, which are based on nonionic surfactants and neutral inorganic precursor. In 1998, hexagonal array of pores designated as SBA-15 (Santa Barbara Amorphous No 15) was produced with larger pore size and better thermal, mechanical and chemical resistance properties for catalysis applications. Typical synthesis of SBA-15 requires non-ionic triblock copolymer as structure directing agent [21].

Mesoporous silica materials can be synthesized in various forms, such as powders or thin films. Thin films can be coated on various substrates for applications either in catalysis or in drug-delivery devises. Dip-coating and spin-coating are two methods for the synthesis of mesoporous silica thin films. In both methods, a thin film of a precursor solution is formed onto a substrate. The precursor solution contains silica building blocks, such as tetraethyl orthosilicate (TEOS), and surfactant or triblock-copolymers molecules as templates in an acidic ethanol/water solution.

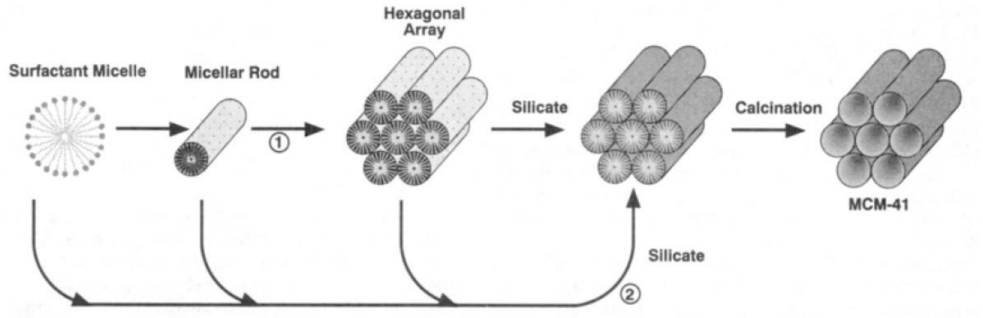

Figure 2: *Schematic show a possible mechanistic for the pathways of the formation of MCM-41: (1) liquid crystal initiated and (2) silicate anion initiated [17]*

The preferential evaporation of ethanol and increasing surfactant concentration in the depositing film leads to a process called Evaporation Induced Self-Assembly (EISA), which results in the organization of silica-surfactant micelles into liquid crystalline mesophases [22]. There are two synthesis mechanisms to explain EISA: a two-step mechanism and a cooperative one-step mechanism. During the formation of mesoporous material following the two-step mechanisms, the surfactant concentration in the precursor solution is below the critical micelle concentration (CMC) resulting in that no micelles of surfactants are formed in the bulk. Solvent evaporation leads to an increase in surfactant concentration and formation of a liquid crystal phase. Finally, a silica framework is formed around the liquid crystalline phase. In contrast, the cooperative one-step mechanism assumes the inorganic silica somehow affects the self-organization of the surfactants into ordered arrays [23]. Different pore topologies (hexagonal, cubic, and lamellar) can be obtained depending on the silica to surfactant ratio.

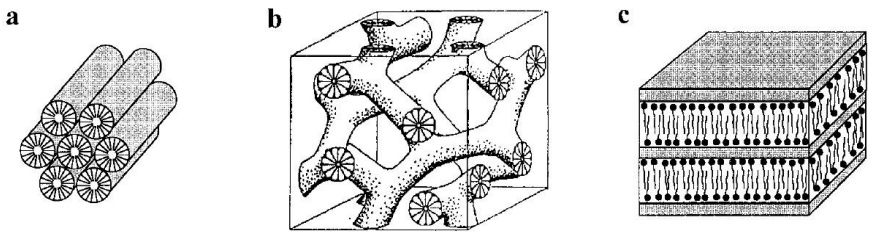

Figure 3: *Three structure types observed for silica-surfactant mesophases: (a) hexagonal (MCM-41); (b) cubic bicontinuous (MCM-48) and (c) lamellar (MCM-50)[24]*

1.3. Dendrimers

Dendritic patterns are perhaps one of the most common topologies seen on the earth. Countless examples of this architecture are found both in the abiotic world (e.g., lightning patterns, snow crystals, and erosion fractals), as well as in the biological systems (e.g., tree branching/roots, plant/animal vasculatory systems, and neurons). The first laboratory synthesis of such dendritic pattern occurred in the late 1970s to the early 1980s when a new core-shell molecular architecture was synthesized, which is now known as "dendrimers" [25].

Dendrimers belong to the so called fourth polymeric structural classification "dendritic architecture", which includes random hyperbranched polymers, dendrigraft polymers and dendrons besides dendrimers. Four subsets of dendritic architecture are listed in increasing order related to the degree of structural control in Figure 4 [26]. Dendrimers are a class of synthetic regularly branched, highly monodisperse spherical molecules with a well-defined covalent connectivity. Their molecular architecture consists of a core, regularly branching repeat units and terminal groups [27]. Dendrimers have been used in a wide range of applications due to their extraordinary structure and they have been employed in different fields, including magnetic resonance imaging, drug delivery, gene therapy, chemical separation, sensors, nanoreactors, and catalysis [28, 29]. Dendrimers are produced in a repetitive sequence of reaction steps, where each step involves covalently attachment of molecule forming a new layer on top of the previous layer. This is referred as formation of a higher generation dendrimer. Each successive generation results in a dendrimer with double the number of end groups (active sites) and roughly twice the molecular weight of the previous generation. The relatively simple and accurate control of the size, composition, and chemical reactivity of dendrimers is one of the most interesting aspects of these materials [30].

Polyamidoamine (PAMAM) dendrimers were the first complete dendrimer family to be synthesized, characterized and commercialized and thus they are the most widely studied dendrimers [31]. These dendrimers are hydrophilic macromolecular polymers consisting of a core of ammonia or ethylenediamine molecules that is surrounded by amidoamine molecules as branching units. The branching units have either primary amine (full generation i.e. G1, G2, etc.) or methyl esters (half generation i.e. G0.5, G1.5, etc.) as terminal groups [32].

Since it has been shown that amine-terminated PAMAM dendrimers adsorb very strongly to silica surfaces [29], these are considered to be promising to use in the investigation of the mass sensitivity of different silica surfaces (non-porous and mesoporous silica having different pore sizes). The other advantages of PAMAM dendrimers to be used in the study are their monodispersity and availability in different sizes.

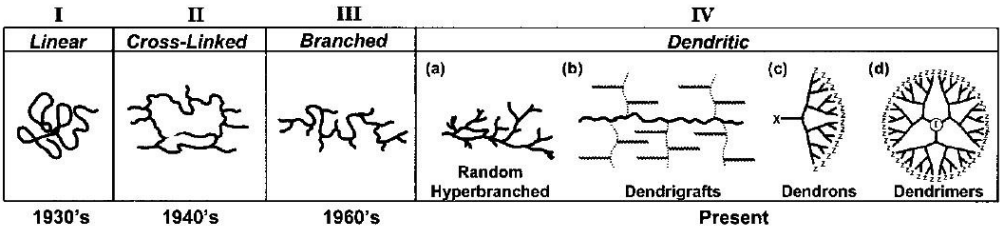

Figure 4: *Representation of the four major classes of polymeric architectures[26]*

2. Materials and Methods

2.1. Synthesis of Mesoporous Silica Films

In this study three different types of mesoporous silica thin films having varying pore sizes have been synthesized. The mesoporous silica structures were templated by cationic and nonionic surfactants, CTAB and Brij S10, respectively, as well as by the nonionic triblock co-polymer Pluronic P123.

CTAB templated mesoporous silica sols were prepared according to a method reported in the literature [33]. In a typical preparation, 4.52 g tetraethyl orthosilicate [TEOS, $Si(OC_2H_5)_4$, reagent grade, 98%, Sigma-Aldrich], 1.94 g Milli-Q water (18 MΩcm Resistivity, collected from Branstead E-pure filtration system adjusted to pH~1.25 with HCl (ACS reagent, 37%, Sigma-Aldrich)) and 3.80 g ethanol (99.5 v%, Kemetyl AB, Sweden) were mixed by magnetic stirring at 20 °C for 30 minutes. The silica sol was then aged at 40 °C for 90 minutes. This was followed by preparation of a solution containing 1 g CTAB (Cetyltrimethylammonium bromide, $CH_3(CH_2)_{15}N(Br)(CH_3)_3$, Sigma-Aldrich) dissolved in 6.20 g ethanol that was mixed with the aged sol by magnetic stirring for 30 minutes at 20 °C. Finally thin films were formed on AT-cut sensor crystals or glass slides by spin-coating at 400 rpm for 10 s followed by 4000 rpm for 60 s. Prior to spin-coating the substrates were cleaned in SDS solution (2 wt %) and ultra-pure Milli-Q water for 15 min each, then dried in a flow of nitrogen gas. The prepared thin films were then aged under room temperature and humidity condition for 24 h. Finally the thin films were calcined by heating at a rate of 1 °C/min up to 400 °C and holding for 4 h to remove the organic species and increase the cross-linking of the inorganic framework.

Synthesis of mesoporous silica using Brij S10 was based on the method developed by Jung et al. [34]. In a typical preparation, 5.90 g TEOS, 0.60 g dilute HCl (pH 2.6), and 5 g ethanol were mixed by magnetic stirring at 60 °C for 90 minutes. Then a solution of 1 g Brij S10 (Polyethylene glycol octadecyl ether, $C_{18}H_{37}(OCH_2CH_2)_nOH$, n~10, Sigma-Aldrich) dissolved in 2 g ethanol was prepared and mixed with the silica sol by magnetic stirring for 24 hours at 20 °C. Thin films were then formed as described above.

Mesoporous silica templated by Pluronic P123 was prepared according to a method reported in the literature [35]. In a typical preparation, 6.13 g TEOS, 3.18 g dilute hydrochloric acid (pH 2), and 4.72 g ethanol were mixed by magnetic stirring at 20 °C for 20 minutes. Then a solution of 1 g Pluronic P123 (Poly(ethylene glycol)-block-poly(propylene glycol)-block-poly(ethylene glycol), $EO_{20}PO_{70}EO_{20}$, Sigma-Aldrich) dissolved in 4.72 g ethanol was mixed. The silica sol was then aged for one hour in a fridge (12 °C) followed by spin-coating as described above.

2.2. Materials characterization

2.2.1. Surface Area and Pore Structure

The pore characteristics of solids can be characterized by different techniques. One common technique to be used is the physical gas adsorption in which a gas (N_2, Ar, or CO_2) is adsorbed on a solid material. In this method the amount of adsorbed gas is considered as a direct measure of the properties and structure of the pores. Advantages of the technique are that it is relatively fast and easy to use. Information on the surface area, pore volume, and pore size distribution (PSD) can be determined by the obtained isotherm from the adsorption-desorption measurements [36].

Figure 5 shows the six types of adsorption-desorption isotherms according to International Union of Pure and Applied Chemistry (IUPAC). Type IV isotherm is characteristic for mesopores materials, which has a hysteresis loop that is related to capillary condensation of the gas. The hysteresis loops have different shapes (Fig. 6). The Type H1 is characteristic for porous materials consisting of agglomerates or uniform spheres compacted approximately in a regular array with narrow distributions of pore size. The Type H2 is observed for mesoporous material having an undefined distribution of size and shape of the pores (many porous adsorbents e.g. inorganic oxide gels and porous glasses). The Type H3 loop does not show any adsorption limit at high P/P_0, which is associated with slit-shaped pores due to aggregates of plate-like particles. Finally, the Type H4 loop is often observed with

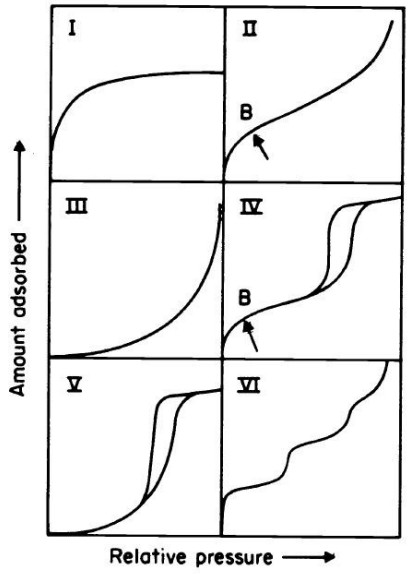

Figure 5: *Types of adsorption-desorption isotherms [37]*

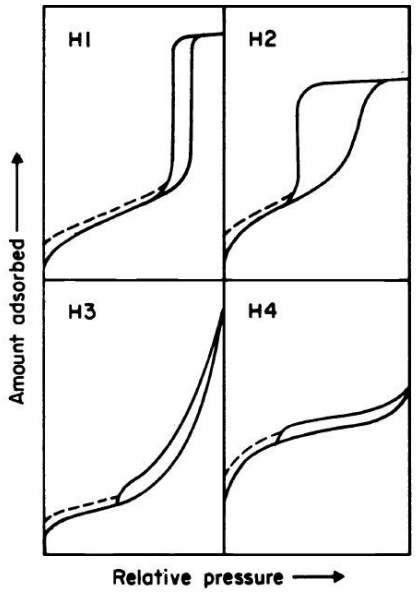

Figure 6: *Types of hysteresis loops [37]*

narrow slit-like pores, however this case with the Type I isotherm is characteristic of microporosity [37].

Nitrogen adsorption–desorption isotherms for the different mesoporous materials were measured using a Micromeritics TriStar 3000 instrument (Georgia, US) operated at liquid nitrogen temperature (77 K). The samples were prepared by scraping off silica material from glass substrates (20×10 cm). Prior to analysis all samples were degassed at 200 °C for 3 h under vacuum pressure. The specific surface areas were calculated using the Brunauer-Emmett-Teller (BET) method in the range of relative pressure from 0.04 to 0.20. The cumulative volumes of the pores were determined from adsorption at 0.98 P/P0. Pore size distributions and average pore diameters were calculated using the Barret-Joyner-Halenda (BJH) model on the adsorption branch of the adsorption-desorption isotherms.

2.2.2. Transmission electron microscopy (TEM)

Transmission electron microscope (TEM) has been a key analytical tool in the characterization of mesoporous materials. The basic principles on which TEM operates are the same as for light microscopes. The main difference is that TEM uses electrons instead of light to visualize the sample. Electrons have a much shorter wavelength than light, which gives a thousand times better resolution in TEMs compared to in light microscopy. In TEM a beam of electrons is transmitted through an ultra-thin specimen resulting in projection of an image on a screen based on the interaction of electrons with the specimen. As can be seen in Figure 7, this interaction can produce different signals, which are detected to collect information about the sample [38].

TEM micrographs of mesoporous silica thin films were obtained using a JEM-1200 EX II TEM (Tokyo, Japan) operated at 120kV.

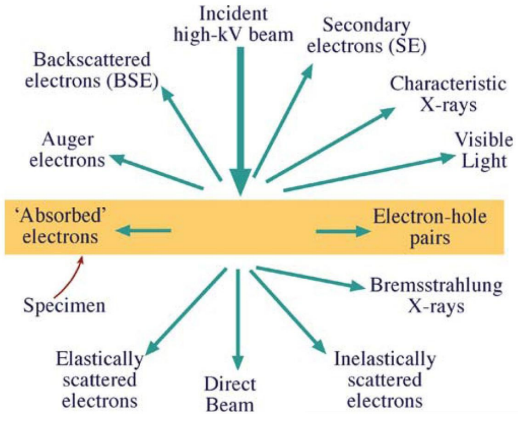

Figure 7: *Signals generated in TEM due to interaction of a high-energy beam of electrons with a thin specimen [38].*

TEM samples were prepared by scratching off mesoporous thin films from the coated glass slides and then dispersing the sample in ethanol. The dispersion was sonicated for 1 minute. Finally, few drops of the dispersion were added to the holey carbon grid followed by evaporation of ethanol in air.

2.2.3. Dynamic light scattering (DLS)

Dynamic Light Scattering (DLS), also known as Photon Correlation Spectroscopy or Quasi-Elastic Light Scattering, is one of the most widely used methods to measuring the size of particles. This technique uses a monochromatic light beam, such as a laser, to measure the random movement of particles (Brownian motion) in a solution. The wavelength of the incoming light changes upon interaction with particles in the solution. The result is dependent on the size of the particle. The collected data is then used to calculate the size distribution of the particles [39].

DLS measurements were carried out using a Zetasizer nano- ZS, Malvern instruments (Worcestershire, UK).

2.3. Quartz crystal microbalance with dissipation monitoring (QCM-D)

QCM-D measurements were performed on a Q-Sense E4 instrument (Q-Sense AB, Gothenburg, Sweden), which was equipped with a QAFC 301 axial flow chamber. AT/cut piezoelectric quartz crystals (14 mm, 5 MHz) coated with silica (Q-Sense AB, Gothenburg, Sweden) was used in the analysis. Some of the crystals were coated with mesoporous silica having varying pore size as discussed previously.

The QCM-D measurements are carried out by applying an electrical field over the quartz crystals, which results in that the crystal starts to oscillate at its own frequency until stable baselines is obtained. The oscillation frequency changes upon adsorption of different substances. The change in frequency due to the mass of the adsorbate is then used to study the adsorption behavior of a substance.

In this study, the first four generations (G0, G1, G2, and G3) of PAMAM dendrimers (20 wt. % in methanol, Sigma Aldrich) having ethylenediamine core and amine terminal groups (Fig. 8) were used as the adsorbate.

In this project the adsorption of 0.1 wt. % solutions of PAMAM G0, G1, G2, and G3 dispersed in methanol (ACS reagent, Sigma-Aldrich) or Milli-Q water on mesoporous and non-porous silica was investigated.

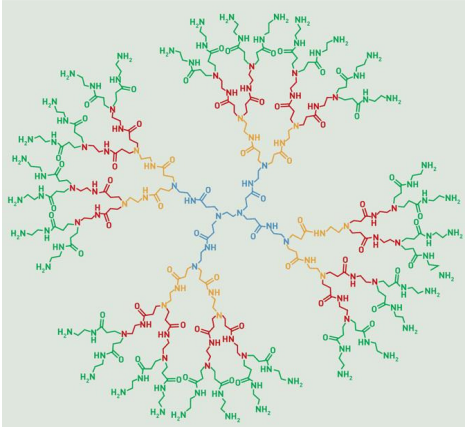

Figure 8: *Molecular scheme illustrates the third generation (G3) PAMAM dendrimer having ethylenediamine core (blue). Each color shows a successive generation [40].*

Table 1 shows the calculated properties of these dendrimers according to specifications [41]. Furthermore, the adsorption of ions (NaCl, KCl (GR for analysis, Merck), and $CaCl_2$ (Aldrich): 10 mM), Dimethylamine (40% in water, Fluka), tetra ethylene glycol (99%, Aldrich): and Sodium alendronate dispersed in water on mesoporous and non-porous silica was investigated.

Prior to QCM-D analysis the crystals were cleaned by UV for 2 hr, followed by immersion in SDS solution (2 wt. %) for 1.5 hr , rinsing in Milli-Q water stream for 1 hr. The surfaces were than dried with nitrogen gas and then put in the UV for 10 min.

Table 1: *The calculated properties of PAMAM dendrimers*

Generation	Molecular Weight	Measured Diameter (nm)	Surface Groups
G0	517	1.5	4
G1	1,430	2.2	8
G2	3,256	2.9	16
G3	6,909	3.6	32

3. Results and Discussion

3.1. Transmission Electron Microscopy (TEM)

Cubic mesoporous silica was successfully synthesized according to TEM micrographs, as is seen in Figure 9. From the micrographs the pore diameters were measured to be roughly 3 and 5 nm for mesoporous silica prepared using Brij S10 and P123 as template agent, respectively. However, the pore diameter for mesoporous silica prepared using CTAB as template agent could not be obtained (Fig. 9a). The measured pore sizes were similar to the numbers obtained using nitrogen adsorption (see Table 2).

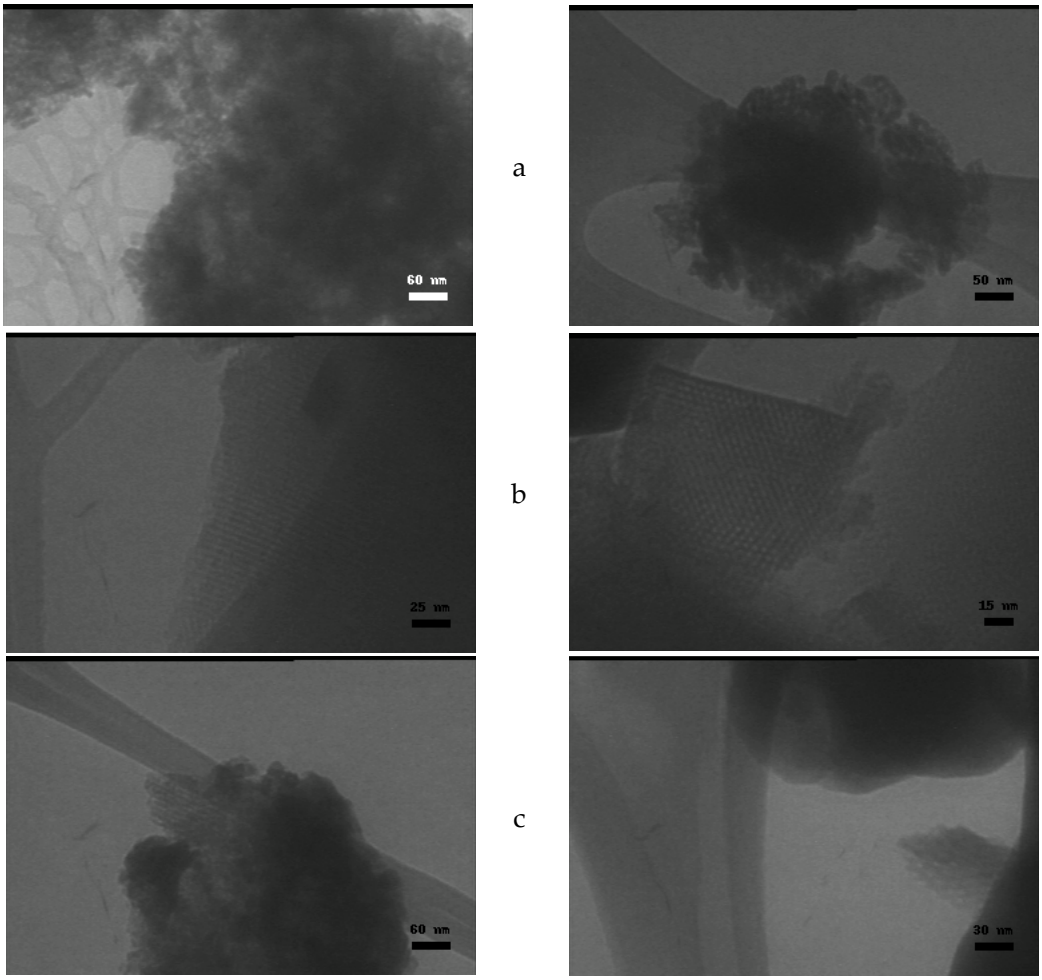

Figure 9: *TEM images of mesoporous silica thin films prepared using (a) CTAB, (b) Brij S10, and (c) Pluronic P123 as templating agents.*

3.2. Nitrogen adsorption

Nitrogen adsorption was used to measure the surface area, pore volume and pore size distribution (PSD) of the synthesized mesoporous silica thin films. Figure 10 shows nitrogen sorption isotherms for mesoporous silica templated by CTAB, Brij S10, and Pluronic P123, respectively. All three materials exhibited nitrogen adsorption–desorption isotherms and hysteresis loops of type IV, which confirms the presence of mesoporous structure. BET specific surface areas, cumulative volumes of the pores and average pore diameter for the synthesized materials were calculated from the isotherms and are summarized in Table 2.

For mesoporous silica prepared using CTAB as template agent, a narrow hysteresis loop of type H1 with parallel adsorption and desorption branches were observed, which had a well-defined step in the relative pressure range of P/P_0 0.22-0.32 (Fig. 10a). This indicated that the pores had a narrow size distribution. The calculated surface area, pore volume and pore diameter for this material were similar to values reported by Zhang et al. [42]. The isotherm for Brij S10 templated mesoporous silica (Fig. 10b) showed a hysteresis loop of type H2 with pore condensation in relative pressure range below 0.4. This is believed to be due to the existence of micro- and mesopores in the material. The t-plot micropore volume was calculated to be 23 mm^3/g. As can be seen in Figure 10c, the P123 derived mesoporous silica had a H2-type hysteresis loop, which indicated that the pore size distribution and pore shape were not well-defined. The pore condensation occurred in relative pressure range of P/P_0 0.61-0.72 and the t-plot micropore volume was calculated to be 54 mm^3/g. The calculated BET surface areas and pore volumes for mesoporous silica prepared using Brij S10 and P123 as tremplate agents were lower compared to those reported in the literature [42].

As expected from classical theories, the pore condensation occurred at higher relative pressures with increasing pores size [43].

Table 2: *The physicochemical properties of the synthesized mesoporous silica materials prepared using CTAB, Brij S10 and P132 as template agents obtained using nitrogen adsorption.*

	BET Surface Area (m^2/g)	Total Pore Volume (mm^3/g)	Pore Diameter (nm)
CTAB templated	733	448	2.4
Brij S10 templated	232	143	3.1
Pluronic P123 templated	249	205	5.2

a)

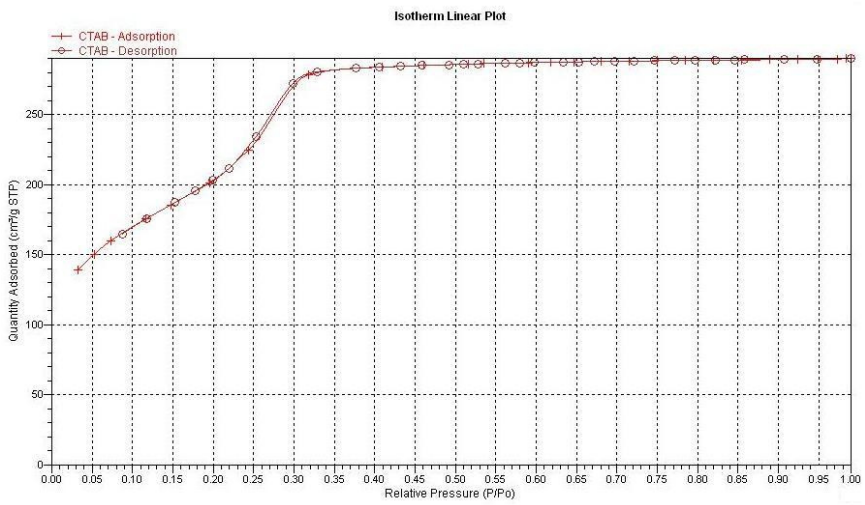

b)

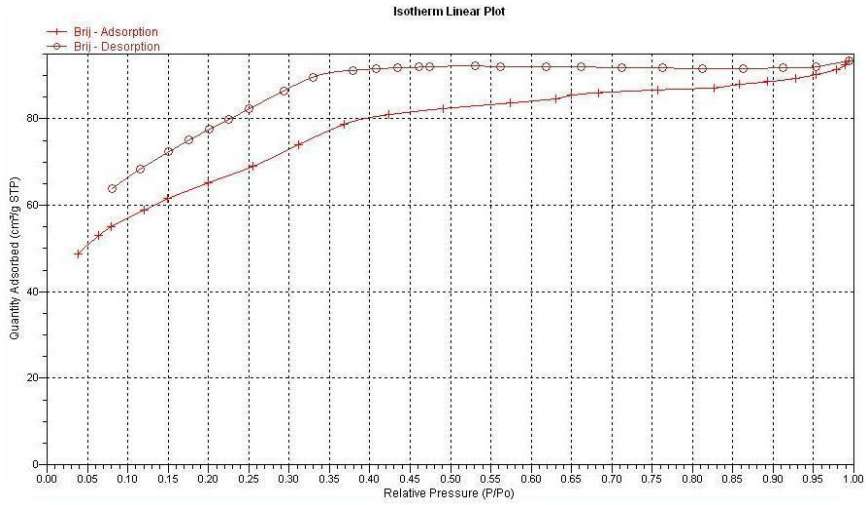

c)

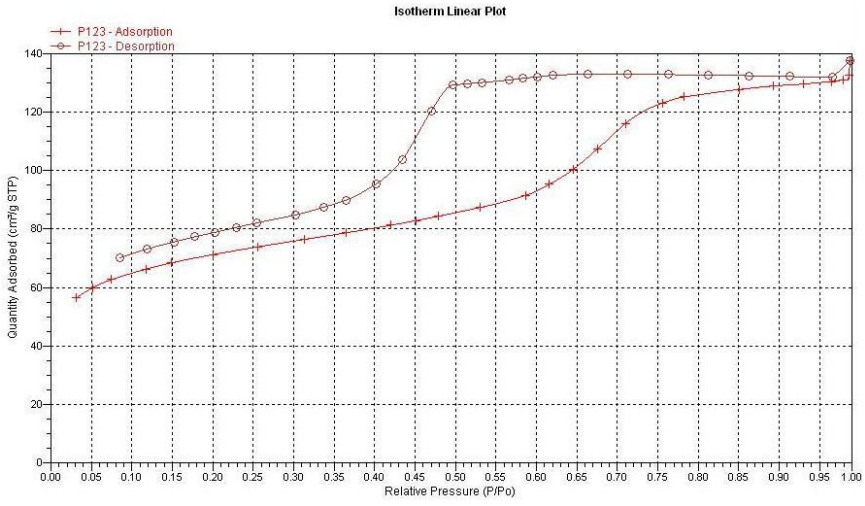

Figure 9: *Nitrogen adsorption–desorption isotherms for mesoporous silica prepared using (a) CTAB, (b) Brij S10, and (c) Pluronic P123 as templating agent.*

3.3. Dynamic Light Scattering (DLS)

The size distributions of different generations of PAMAM dendrimers dispersed in methanol and water measured using DLS (Fig. 11).

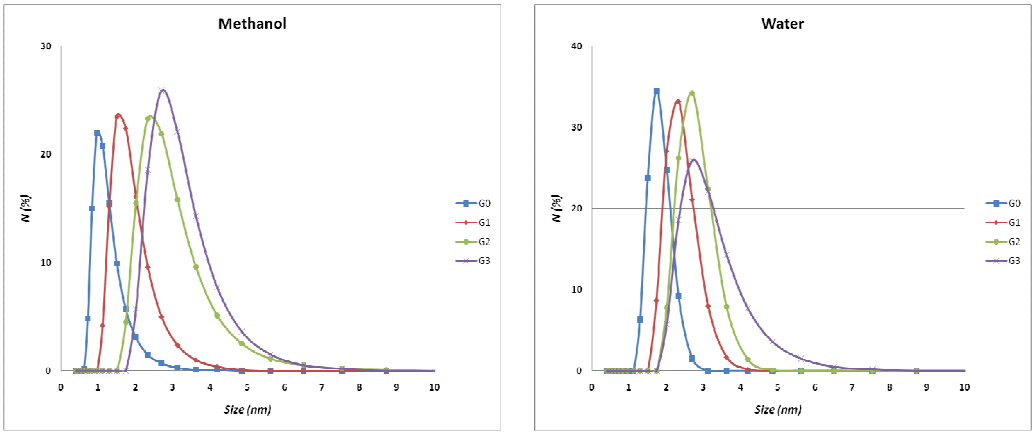

a b

Figure 11: *DLS measurements show distribution function of the diameter of PAMAM dendrimers (G0, G1, G2, and G3) dispersed in (a) methanol and in (b) fresh water solutions*

The measured number mean sizes of the dendrimers are shown in Table 3. In the Table it can be seen that the measured sizes of dendrimers dispersed in methanol and freshly dispersed in water were comparable with the estimated sizes, according to specifications (see Table 1). However, the dendrimers that were dispersed in water a week before analysis were observed to be much larger. This is believed to be due to aggregation of dendrimers resulting in formation of large clusters.

Table 3: *The mean number molecule diameter for different generations of PAMAM dendrimers dissolved in methanol and water obtained using DLS.*

Generation	Diameter (nm) in methanol solution	Diameter (nm) in freshly prepared water solution	Diameter (nm) in one week aged water solution
G0	1.2	1.9	42.6
G1	1.8	2.4	149.4
G2	2.8	2.7	-
G3	3.1	3.2	-

3.4. Adsorption behavior of mesoporous silica thin films prepared using CTAB as templating agent

3.4.1. Adsorption of PAMAM dendrimers dispersed in methanol

QCM-D was used to compare the adsorption behavior of PAMAM dendrimers on non-porous (NP) and mesoporous silica coated sensor crystals. Figures 12 to 15 show the frequency changes at three different overtones (3rd, 5th, and 7th) upon adsorption of PAMAM dendrimers on the different crystals.

The graphs in Figure 12 illustrate the adsorption behavior of PAMAM G0 dendrimers in two different runs using different coated crystals prepared from the same precursor solution. As can be seen in Figure 12a the frequency shift describing the adsorption of dendrimers on non-porous silica was less than 20 Hz and in the range of 160-180 Hz on mesoporous silica. Same experiment shown in Figure 12b gave a frequency shift of 8 Hz on non-porous silica and in the range of 235-250 Hz on mesoporous silica; this indicated that the sensitivity increased 30 times for the mesoporous coated crystals.

In Figure 13, the differences in adsorption of PAMAM G1 dendrimers on non-porous and mesoporous silica coated crystals are presented. The results in Figure 13a show that the frequency shift for dendrimer adsorption on mesoporous silica was about twice as large as dendrimer adsorption on non-porous silica. According to Fig. 13b the adsorption of dendrimers was about 3 to 4 times larger compared to results presented in Fig. 13a.

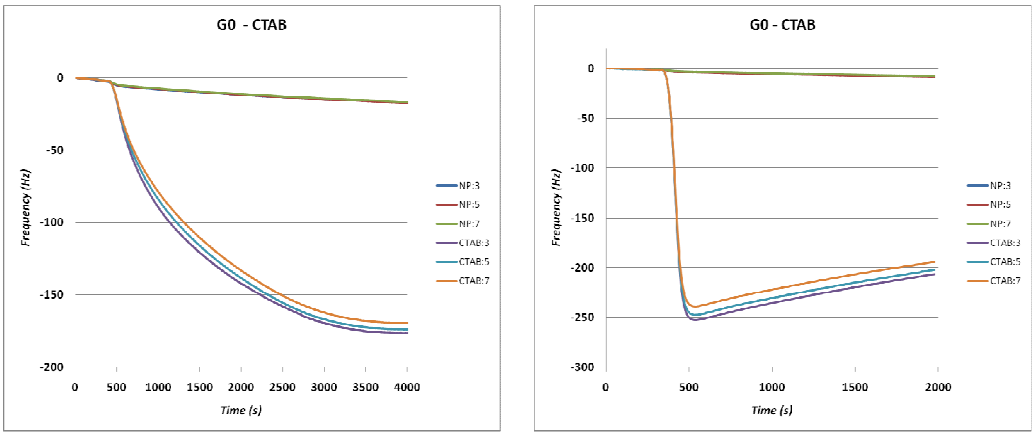

a b

Figure 12: *QCM-D measurements presented as shifts in frequency (Δf) show adsorption of PAMAM G0 dendrimers dissolved in methanol on non-porous and mesoporous silica prepared using CTAB as template. (a) and (b) show results from dendrimer adsorption on two different mesoporous silica coated crystals. The used dendrimer solution was the same in both experiments.*

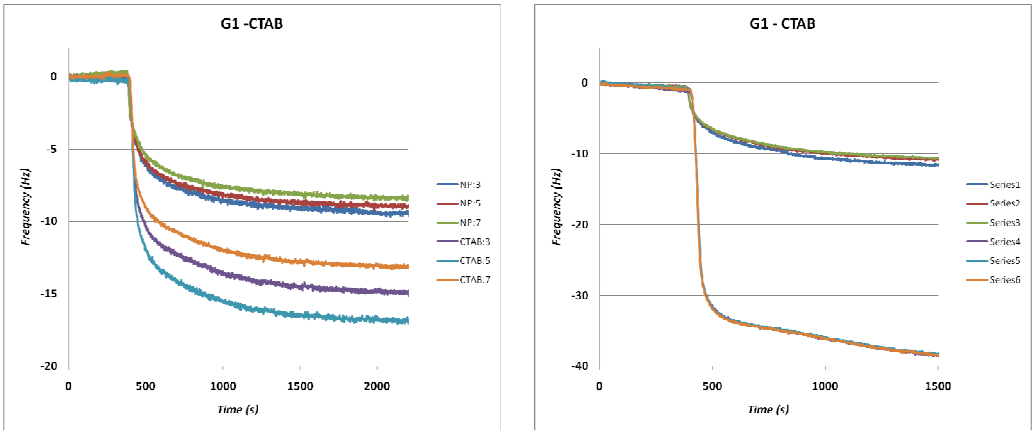

a b

Figure 13: *QCM-D measurements presented as shifts in frequency (Δf) show adsorption of PAMAM G1 dendrimers dissolved in methanol on non-porous and CTAB- derived mesoporous silica. (a) and (b) show results from experiments preformed on two different mesoporous coated crystals.*

In both experiments the crystals were coated with mesoporous silica prepared from the same precursor solution. The observed difference in result could be due to the spin-coating process. However, in both experiments the frequency shift representing the adsorption of G1 dendrimers was lower than the frequency shift illustrating the adsorption of G0 dendrimers on mesoporous silica (see Fig. 12). One explanation for the observation could be due to the size difference of the PAMAM G0 and G1 dendrimers (see Table 3). The small G0 dendrimers are believed to get access to the internal surface of pores, whereas the larger G1 dendrimers are suggested to be too large to get into the pores and consequently adsorb on the surface of the mesoporous material. The increased adsorption of G1 dendrimers on mesoporous silica compared to non-porous silica is suggested to be related to the surface roughness of mesoporous silica.

QCM-D measurements in Fig. 14 show the adsorptions of PAMAM G2 dendrimers on non-porous and mesoporous silica. According to the results the frequency shifts observed on mesoporous silica were about twice as high as those obtained on non-porous silica.

Again, the possible reason for these differences can be due to differences in roughness of the different surfaces. Furthermore the size of the dendrimers (~ 2.8 nm) is larger than the estimated pore size (2.4 nm) of the mesoporous silica surface, which results in that the dendrimers are not able to access the internal surface of the pores. The decreased adsorption of G2 compared to G1 dendrimers on mesoporous silica indicated that the adsorption was dependent on the size of the dendrimers.

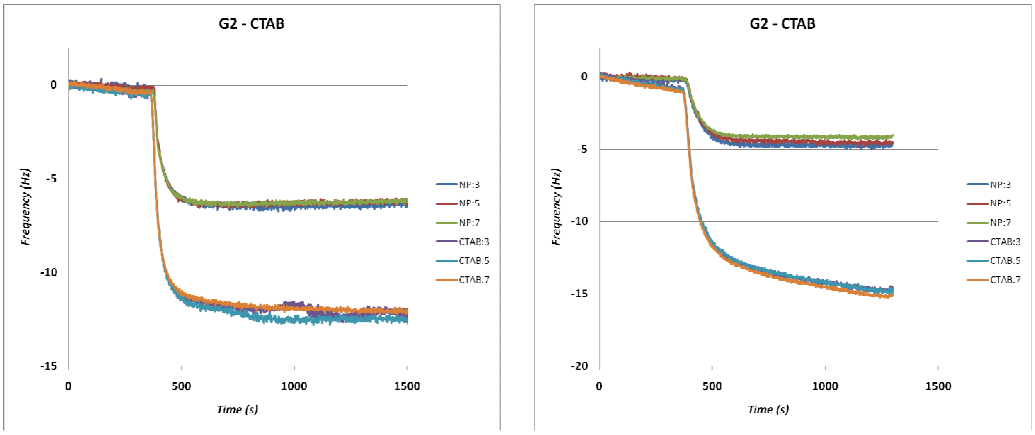

a b

Figure 14: *QCM-D measurements presented as shifts in frequency (Δf) show adsorption of PAMAM G2 dendrimers dissolved in methanol on non-porous and CTAB- derived mesoporous silica. (a) and (b) represent adsorption of dendrimers on two different sets of crystals.*

Surprisingly, the frequency shift observed for the adsorption of PAMAM G3 dendrimers on mesoporous silica was much larger compared to the obtained frequency shift for the adsorption of G2 and G1 dendrimers. This is presented in Figure 15a as a shift in frequency of about 73-77 Hz for the different overtones on mesoporous silica compared to 4-6 Hz on non-porous silica. Accordingly, the adsorption of G3 dendrimers was roughly 20 times larger on mesoporous silica than on non-porous silica.

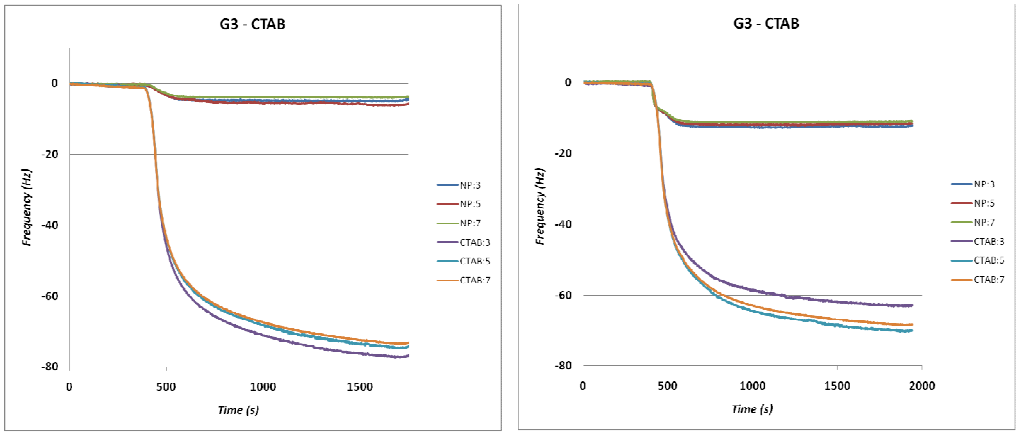

a b

Figure 15: *QCM-D measurements presented as shifts in frequency (Δf) show adsorption of PAMAM G3 dendrimers dissolved in methanol on nonporous and CTAB- derived mesoporous silica. (a) and (b) show the same experiment but using two different batches of crystals.*

One explanation for the obtained result could be due to the higher number of surface groups on G3 dendrimers compare to G0, G1 and G2 dendrimers leading to stronger interaction with the mesoporous silica surface. Esumi et al. showed that the adsorption of PAMAM dendrimers on silica surfaces increases with increasing generation of dendrimers. Their results suggested that the affinity between low generation dendrimers (G0 and G1) and silica surfaces is relatively low [44]. Another explanation could be due to the size of the G3 dendrimers (3.1 nm). Larger molecules give rise to larger frequency shifts upon adsorption on QCM-D crystal. Furthermore, the differences observed in frequency shifts between non-porous and mesoporous silica in the experiment showed in Fig. 15b was three times less than the results presented in Fig. 15a. The frequency shifts for mesoporous silica were 63-70 Hz, which was roughly 6 times larger compare to the frequency shifts obtained on non-porous silica (11-12 Hz). This difference (about three times) could be due to the cleaning procedure of the crystals between the two experiments.

As described previously, the dendrimers were removed from the surfaces by UV treatment followed by rinsing in SDS solution and Milli-Q water. The results indicated that the cleaning procedure was not sufficient, which implied that dendrimers remained on the surfaces after cleaning. As a consequence a lower amount of dendrimers could adsorb on pre-used surfaces.

3.4.2. Adsorption of PAMAM dendrimers dispersed in water

The adsorption of PAMAM G0 and G3 dendrimers dispersed in water on mesoporous silica was investigated using QCM-D. Figures 16-17 show the frequency changes at three different overtones (3^{rd}, 5^{th}, and 7^{th}) upon the addition of dendrimers dispersed in water (0.1 wt. %) on non-porous (NP) and mesoporous silica coated crystals.

In Figures 16a and 16b same pattern for the adsorption of G0 dendrimers was shown for two different runs. Upon the addition of the dendrimer solution, a rapid adsorption was first observed, followed by a strong and positive shift in frequency. The shift in frequency was observed to be much larger on mesoporous silica compared to on non-porous silica. One explanation for the observed positive drift in frequency after the addition of dendrimers could be the diffusion of ions in the water solution through the pores of the mesoporous material.

The frequency shifts for the adsorption of dendrimers in these two experiments were different. Although the crystals were not the same, this difference (about three times) could be due to the cleaning procedure between the two experiments, as described previously.

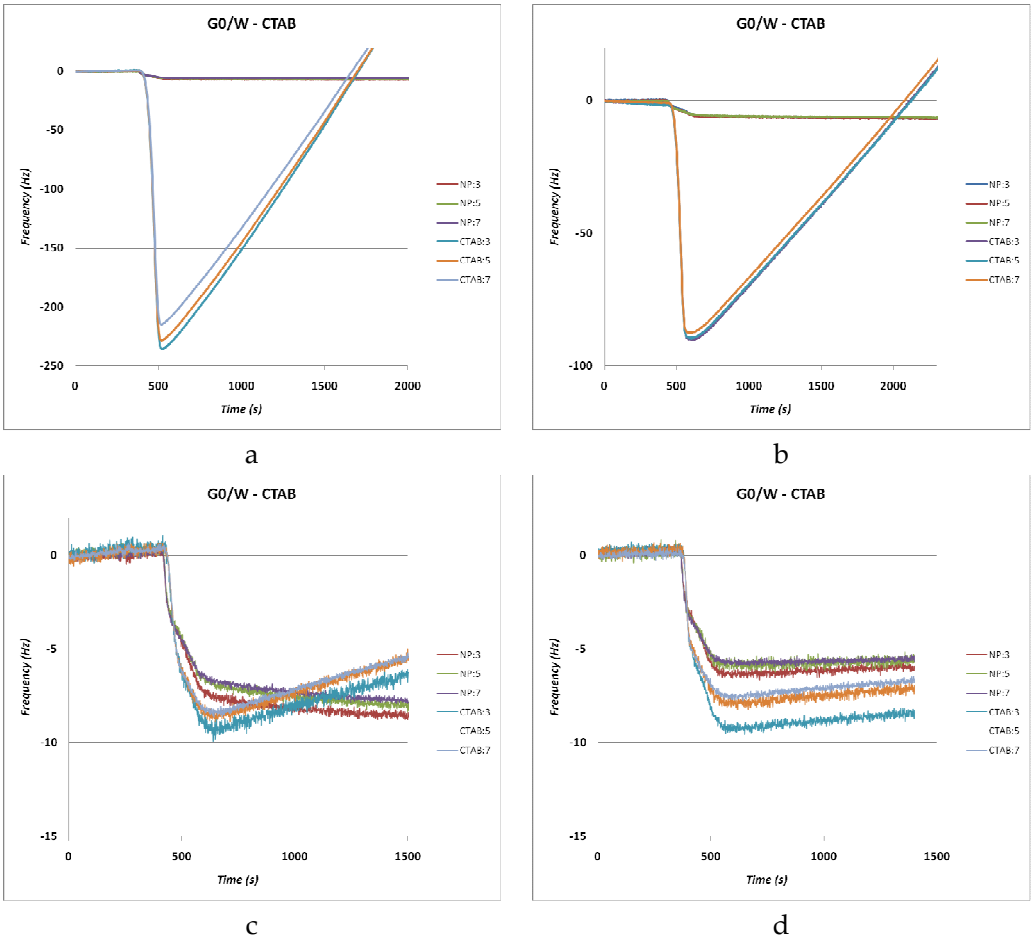

Figure 16: *QCM-D measurements presented as shifts in frequency (Δf) show adsorption of PAMAM G0 dendrimers dissolved in water on non-porous and CTAB-derived mesoporous silica. (a) and (b) show the same experiments using two different batches of crystals and freshly prepared dendrimer solutions. (c) and (d) show the same experiments using aged dendrimer solution*

The dendrimer solutions used in experiments presented in graphs 16a and 16b were freshly prepared whereas the results presented in graphs 16c and 16d were performed with dendrimer solutions that had been aged for one week.

According to the results, the frequency shifts obtained for the adsorption of aged PAMAM G0 dendrimer solution was similar on non-porous and mesoporous silica. The explanation for the results could be due to the aggregation of dendrimer molecules in water during aging, according to Table 3. Consequently, the size of the formed dendrimer clusters was much larger than the size of the pores of the mesoporous silica, which resulted in that the dendrimers adsorbed similarly on both non-porous and mesoporous silica.

The same behavior was observed for G3 dendrimers. Figure 17a illustrates the adsorption behavior of freshly prepared solution of G3 dendrimers in water.

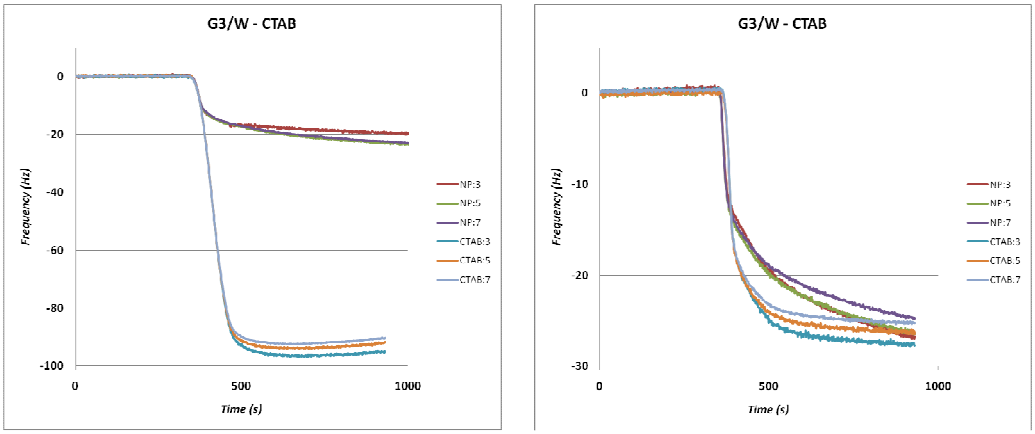

a b

Figure 17: *QCM-D measurements presented as shifts in frequency (Δf) show adsorption of PAMAM G3 dendrimers dissolved in water on nonporous and CTAB-derived mesoporous silica. (a) shows the adsorption of freshly prepared dendrimer solution, and (b) shows the same experiments using aged dendrimer solution.*

The results showed that the frequency shift on non-porous silica was about 25 Hz compared to the frequency change on mesoporous silica, which was about 4 times more (96 Hz).

No difference between the frequency shifts on non-porous and mesoporous silica was observed upon addition of aged G3 dendrimers solution (Fig. 17b). Again the reason for the obtained results could be explained by the aggregation of dendrimers in water upon aging leading to formation of large clusters of dendrimers. Comparing Figures 15 and 17, the frequency shifts representing adsorption of G3 dendrimers dispersed in water were larger on non-porous silica than those obtained after addition of G3 dendrimers dispersed in methanol. The maximum frequency shift was about 10 Hz for dendrimers dispersed in methanol (Fig. 15), compare to about 25 Hz for dendrimers dispersed in water.

3.4.3. Adsorption of other substances dissolved in water

The adsorption of sodium chloride (NaCl), potassium chloride (KCl), calcium chloride ($CaCl_2$), sodium alendronate, Dimethylamylamine (DMA), and Tetra Ethylene Glycol (TEG) dispersed in water on non-porous and mesoporous silica were furthermore investigated. The results (Fig. 18) showed that there was no difference in terms of adsorption for the different molecules on the different surfaces.

In addition, no adsorption was observed for sodium and potassium ions (not shown here) on these two surfaces.

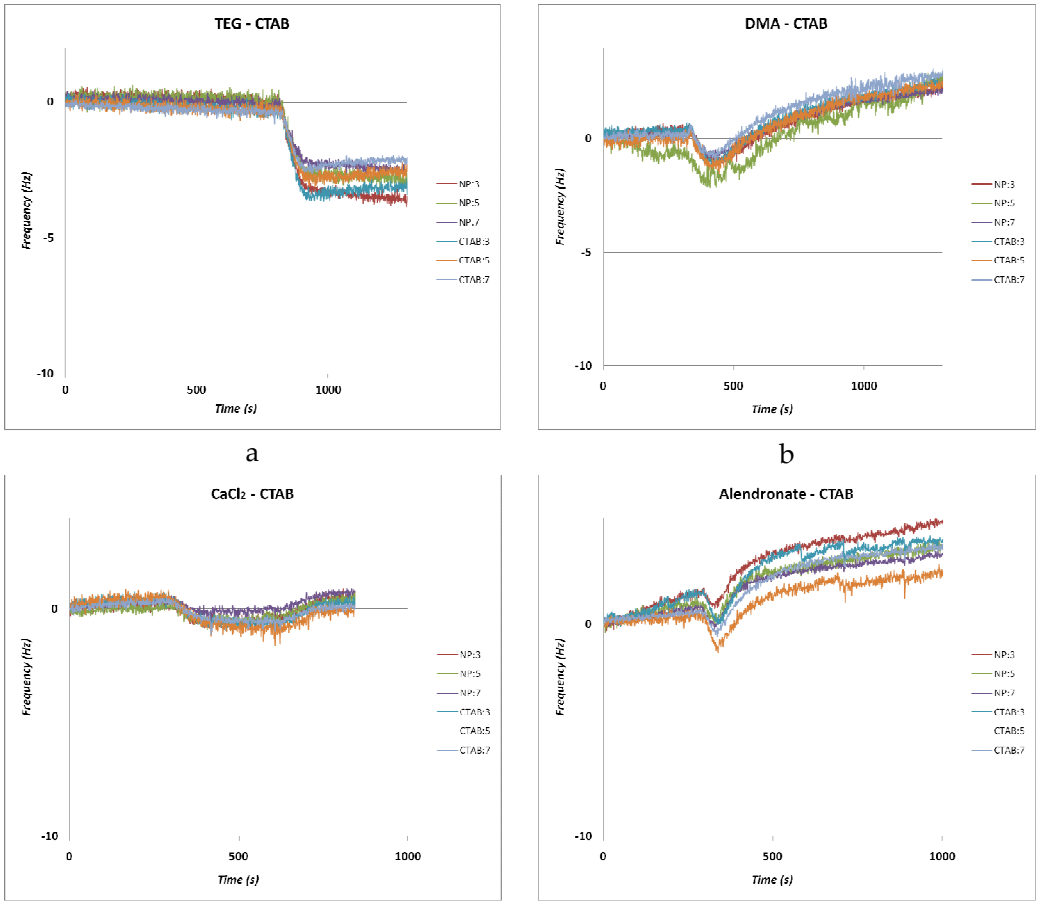

Figure 18: *QCM-D measurements presented as shifts in frequency (Δf) show adsorption of aqueous solutions of (a) Tetra Ethylene Glycol,(b) Dimethylamylamine, (c) calcium chloride, and (d) sodium alendronate on nonporous and CTAB- derived mesoporous silica.*

3.5. Adsorption behavior of mesoporous silica thin films prepared using Brij S10 as templating agent

3.5.1. Adsorption of PAMAM dendrimers dispersed in methanol

QCM-D measurements was performed with the aim to compare the adsorption of G0, G1, G2 and G3 PAMAM dendrimers on nonporous and mesoporous silica prepared using Brij S10 as template agent,. Figures 19 to 22 illustrate the frequency shifts at three different overtones (3rd, 5th, and 7th) caused by the addition of PAMAM dendrimers (0.1 wt. % solution in methanol) on both nonporous (NP) and mesoporous silica coated crystals.

Figure 19 depicts less than 15 Hz shift in frequency on non-porous silica upon adsorption of PAMAM G0 dendrimers followed by a negative drift in frequency for

two different runs. However, the frequency shifts on mesoporous silica (two crystals coated with mesoporous silica using same precursor solution) were about 100 Hz. The observed difference showed that the mesoporosity and its related increased surface area can be used to improve the sensitivity of QCM-D crystal, up to 7 times.

The lower frequency shifts on Brij-templated mesoporous silica surfaces compare to CTAB-derived mesoporous silica surfaces (see Fig. 12) can be explained by its smaller surface area (see Table 2).

The adsorption behavior of G1 dendrimers on non-porous and mesoporous silica coated crystals are presented in Figure 20.

The results in Figure 20 shows that the frequency shifts upon adsorption of dendrimers on mesoporous silica were about 4-5 orders of magnitude higher than the frequency shifts obtained on nonporous silica, in both experiments.

Comparing Figures 19 and 20, it is obvious that the adsorption of G1 dendrimers was lower than the adsorption of G0 dendrimers on mesoporous silica, which according to previously reasoning is due to the difference in size of the PAMAM G0 and G1 dendrimers (see Table 3).

Since mesoporous silica prepared using Brij had larger pores than the CTAB-templated mesoporous silica (see Table 2), both G0 and G1 dendrimers are believed to get access to the internal surface of pores of the mesoporous material. The frequency shifts for the adsorption of G1 dendrimers on CTAB-derived mesoporous silica were 15 and 40 Hz (Fig. 13a and 13b, respectively) and 35 and 50 Hz on Brij S10-derived mesoporous silica, according to Figure 20.

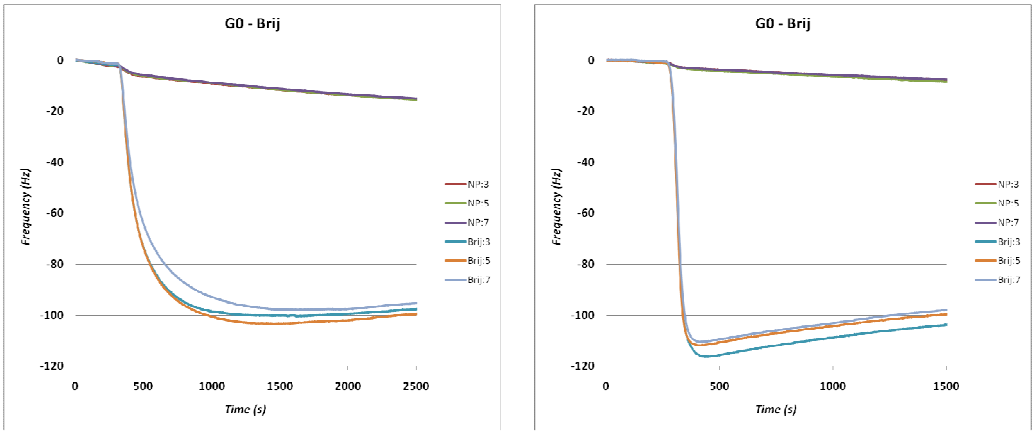

a b

Figure 19: *QCM-D measurements presented as shifts in frequency (Δf) show adsorption of PAMAM G0 dendrimers dissolved in methanol on nonporous and Brij S10-derived mesoporous silica. (a) and (b) show the same experiment but using two different batches of crystals.*

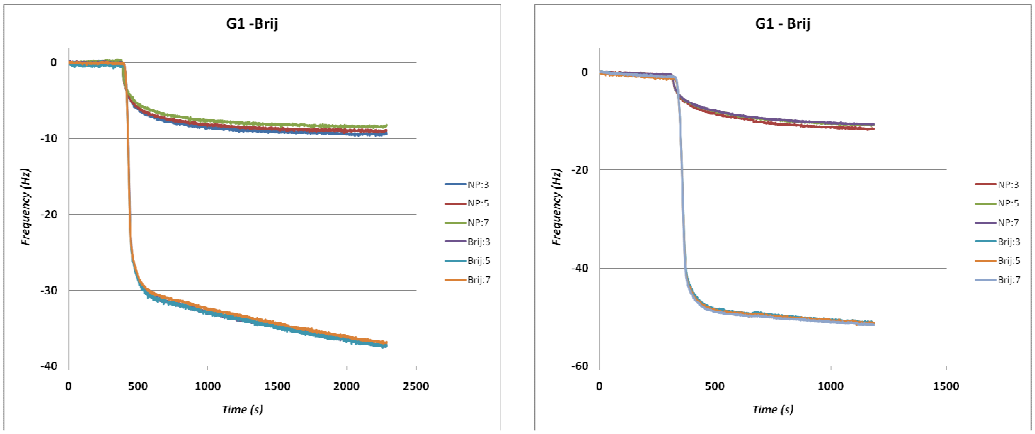

a b

Figure 20: *QCM-D measurements presented as shifts in frequency (Δf) show adsorption of PAMAM G1 dendrimers dissolved in methanol on nonporous and Brij S10-derived mesoporous silica. (a) and (b) show the same experiment but using two different batches of crystals.*

Frequency shifts showing the adsorptions of G2 dendrimers on non-porous and mesoporous silica are presented in Figure 21. In one experiment, the adsorption of dendrimers on mesoporous silica was about 10 orders of magnitude higher than on non-porous silica (Fig. 21a). Another experiment showed a frequency shift of roughly 30 times more for the adsorption of G2 dendrimers on mesoporous silica compare to on non-porous silica (Figure 21b). The observed difference between the two experiments could be due to the cleaning procedure as mentioned previously.

The strange behavior of the adsorption of G2 dendrimers on mesoporous silica, which was larger than observed for G1 and G3 could be explained neither by the surface area of mesoporous silica nor by the dendrimer size.

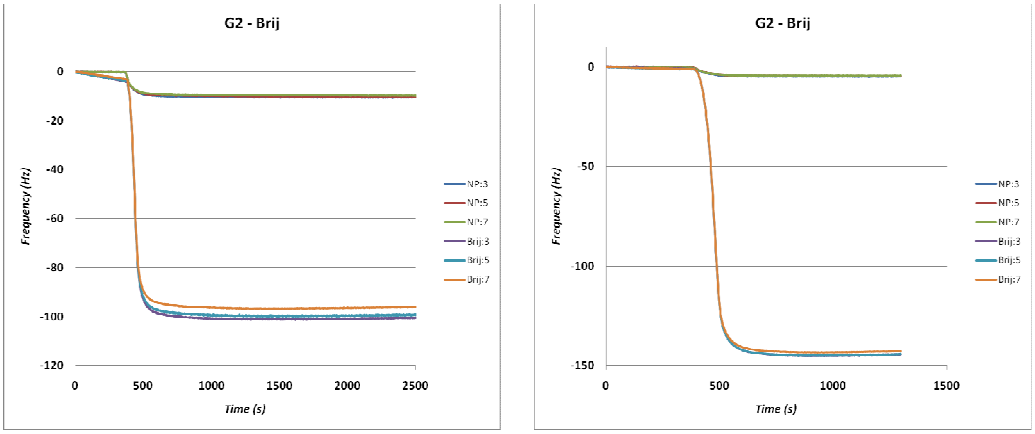

a b

Figure 21: *QCM-D measurements presented as shifts in frequency (Δf) show adsorption of PAMAM G2 dendrimers dissolved in methanol on nonporous and Brij S10-derived mesoporous silica. (a) and (b) show the same experiment but using two different batches of crystals.*

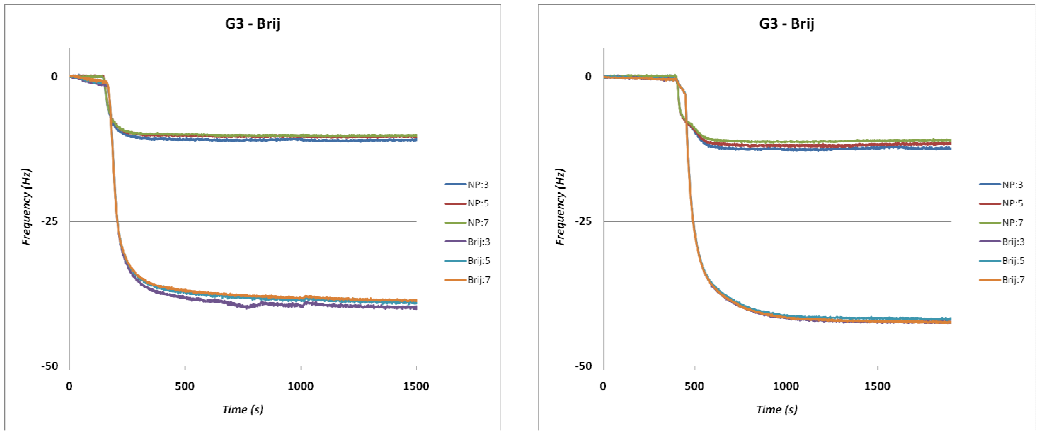

a b

Figure 22: *QCM-D measurements presented as shifts in frequency (Δf) show adsorption of PAMAM G3 dendrimers dissolved in methanol on nonporous and Brij S10-derived mesoporous silica. (a) and (b) show the same experiment but using two different batches of crystals.*

The adsorption of G3 dendrimers on non-porous and mesoporous silica are shown in Figure 22. The frequency shifts on mesoporous silica were about 38-42 Hz for the different overtones compared to 10-12 Hz on non-porous silica (roughly 4 orders of magnitude higher).

The lower frequency shifts on Brij S10-derived mesoporous silica compare to CTAB-derived mesoporous silica (see Fig. 15) can be related to the difference in surface area. The surface area was obtained to be lower for Brij S10-derived mesoporous than for CTAB-derived mesoporous silica (see Table 2), which resulted in a decreased adsorption of G3 dendrimers on Brij S10- derived mesoporous silica.

3.5.2. Adsorption of PAMAM dendrimers dispersed in water

The adsorptions of PAMAM G0 and G3 dendrimers dispersed in water on non-porous (NP) and mesoporous silica synthesized using Brij S10 as template agent were investigated using QCM-D. The frequency shifts at three different overtones (3rd, 5th, and 7th) upon the addition of dendrimers (0.1 wt. % solution in water) on the surfaces are shown in Figures 23-24.

The adsorption pattern for G0 dendrimers on Brij S10-dervied mesoporous silica was similar to that on CTAB-derived mesoporous silica (see Fig. 16). As presented in Figures 23a and 23b, the adsorption of dendrimers dispersed in - fresh water on mesoporous silica showed a rapid drop in frequency (120 and 95 Hz in different runs) followed by a strong and positive shift in frequency. The frequency shift on mesoporous silica was much larger than on non-porous silica (5-7 Hz).

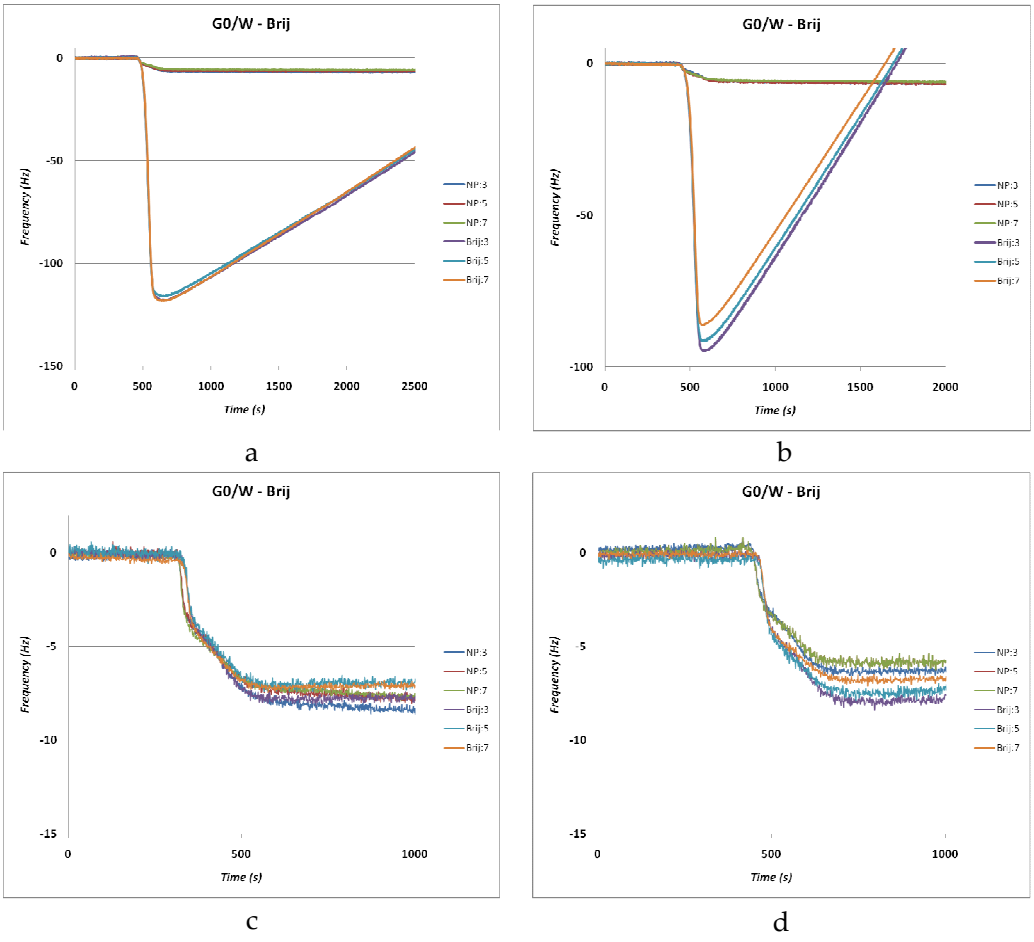

Figure 23: *QCM-D measurements presented as shifts in frequency (Δf) show adsorption of PAMAM G0 dendrimers dissolved in water on non-porous and Brij S10-derived mesoporous silica. (a) and (b) show the same experiments using two different batches of crystals and freshly prepared dendrimer solutions. (c) and (d) show the same experiments using aged dendrimer solution*

The observed drift could be due to the diffusion of ions through the pores to the other side of the crystal. The difference in frequency shifts for the adsorption of dendrimers in these two experiments could be due to the cleaning procedure as discussed previously. The observed decrease in adsorption of G0 dendrimers dispersed in water on Brij S10-dervied mesoporous silica compare to on CTAB-derived mesoporous silica (see Fig. 16a) is believed to be a result of its smaller surface area (see Table 2).

The obtained results for the adsorption of dendrimers, dispersed in water one week before the experiments, on non-porous and mesoporous silica were similar, as can be seen in Figures 23c and 23d. As explained previously, dendrimers dispersed in water are shown to aggregate and form clusters with time; this results in that the formed clusters are much larger than the size of the pores of the mesoporous material leading to similar adsorption behavior on non-porous and mesoporous

silica surfaces (see DLS measurements results, Table 3). Furthermore, no difference was observed in the adsorption of G0 dendrimers, dispersed in water one week before analysis, on mesoporous silica prepared using CTAB or Brij S10 as template agents (see Fig. 16c, 16d, 23c, and 23d).

The adsorptions of G3 dendrimers dissolved in water on non-porous and mesoporous silica are shown in Figures 24a and 24b, respectively. The frequency shifts on mesoporous silica were almost 4 orders of magnitude larger compare to on non-porous silica (Fig. 24a), using dendrimers freshly dispersed in water. Whereas no difference in frequency shifts was observed upon adsorption of G3 dendrimers, dispersed in water one week before analysis, on non-porous and mesoporous silica (Fig. 24b). The possible reason for the obtained results is the aggregation of dendrimers in water during the aging time, as discussed previously.

From the experiments the adsorption of G3 dendrimers dispersed in water was larger than the adsorption G3 dendrimers dispersed in methanol on non-porous silica (compare Fig. 22 and 24).

3.5.3. Adsorption of other substances dissolved in water

The adsorption of sodium chloride (NaCl), potassium chloride (KCl), calcium chloride ($CaCl_2$), sodium alendronate, Dimethylamylamine (DMA), and Tetra Ethylene Glycol (TEG) dispersed in water on non-porous and mesoporous silica were investigated using QCM-D. The results (Fig. 25) showed that there was no significant difference in adsorption of TEG and calcium ions (Fig. 25a and 25c) as well as sodium and potassium ions (not shown here) between non-porous and mesoporous silica.

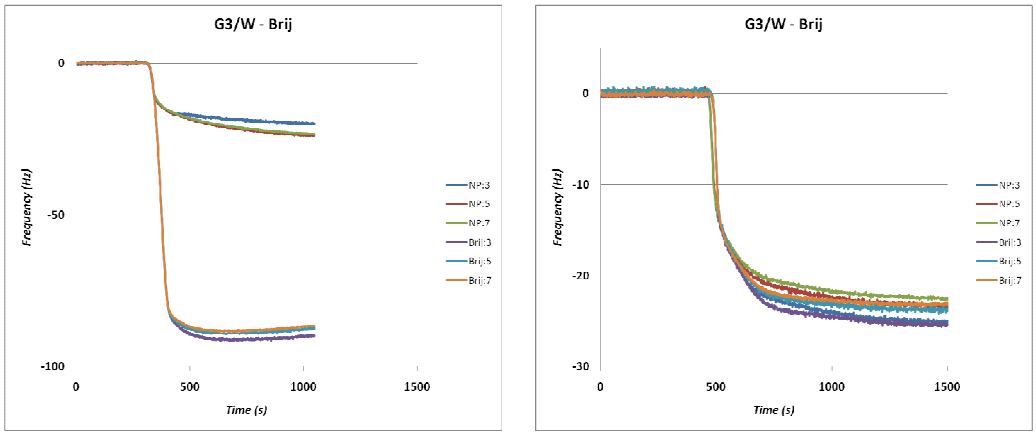

a b

Figure 24: *QCM-D measurements presented as shifts in frequency (Δf) show adsorption of PAMAM G3 dendrimers dissolved in water on non-porous and Brij S10-derived mesoporous silica. (a) shows the adsorption of freshly prepared dendrimer solution, and (b) shows the same experiments using aged dendrimer solution.*

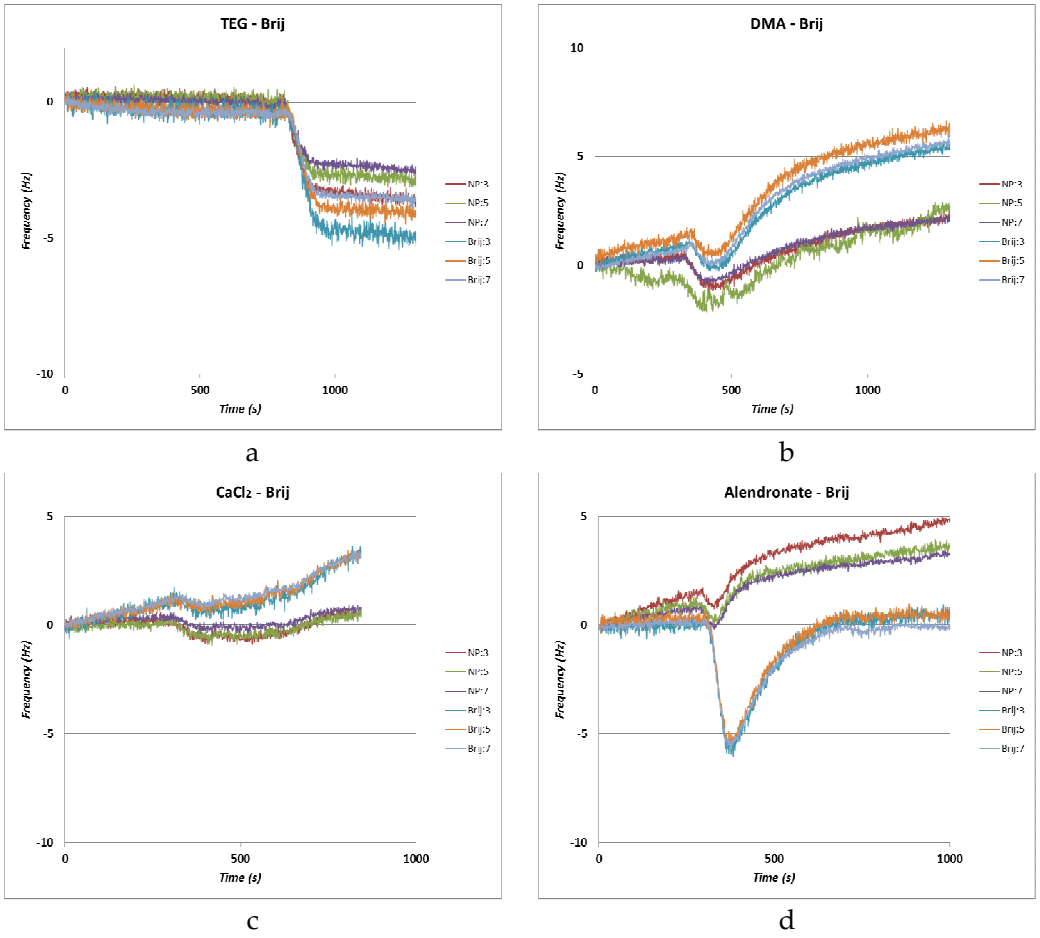

Figure 25: *QCM-D measurements presented as shifts in frequency (Δf) show adsorption of aqueous solutions of (a) Tetra Ethylene Glycol,(b) Dimethylamylamine, (c) calcium chloride, and (d) sodium alendronate on non-porous and Brij S10-derived mesoporous silica.*

However, the observed behavior for the frequency shifts on non-porous and mesoporous silica upon the addition of DMA and alendronate solutions were different (Fig. 25b and 25d).

3.6. Adsorption behavior of mesoporous silica thin films prepared using Pluronic P123 as templating agent

3.6.1. Adsorption of PAMAM dendrimers dispersed in methanol

The adsorption of four different generations of PAMAM dendrimers on mesoporous and non-porous silica was studied using QCM-D. The mesoporous silica prepared using P123 as template had a pore size of 5.2 nm. Figures 26 to 29 show the frequency shifts at three different overtones (3rd, 5th, and 7th) upon the addition of

PAMAM dendrimers (0.1 wt. % solution in methanol) on both non-porous (NP) and mesoporous silica coated crystals.

The results for the frequency shifts on non-porous and mesoporous silica caused by the adsorption of G0 dendrimers are shown in Figure 26. As can be seen in the graphs the maximum frequency shift for different overtones was about 6 Hz on non-porous silica and 95-110 Hz on mesoporous silica. This showed that the sensitivity of the QCM-D crystal was increased by 16-18 orders of magnitude on mesoporous silica compare to non-porous silica.

Comparing these results with previously discussed results for mesoporous silica (prepared using CTAB or Brij S10 as template agent), it can be seen that the frequency shifts on P123-derived mesoporous silica were smaller than those obtained on CTAB-derived or Brij S10-derived mesoporous silica (see Fig. 12 and Fig. 19, respectively). The observed difference in adsorption of G0 dendrimers on P123-derived and CTAB-derived mesoporous silica was believed to be due to the difference in surface area of the two materials. According to Table 2 the surface area was much lower for P123-derived mesoporous silica (as well as Brij S10-derived mesoporous silica) compare to CTAB-derived mesoporous silica. The similar adsorption behavior on mesoporous silica prepared using Brij S10 and P123 confirmed that the adsorption of dendrimers was dependent on the surface area of the material.

The frequency shifts caused by the adsorption of G1 dendrimers on non-porous and mesoporous silica are shown in Figure 27. From the results the frequency shifts were around 9 Hz on non-porous silica and around 230 and 140 Hz on mesoporous silica. The results are given from experiments performed on two different mesoporous silica coated crystals prepared from different precursor solutions (Fig. 27a and 27b). So, an increase in sensitivity of the mesoporous silica coated QCM-D crystals compare to non-porous ones (16-25 times) was observed.

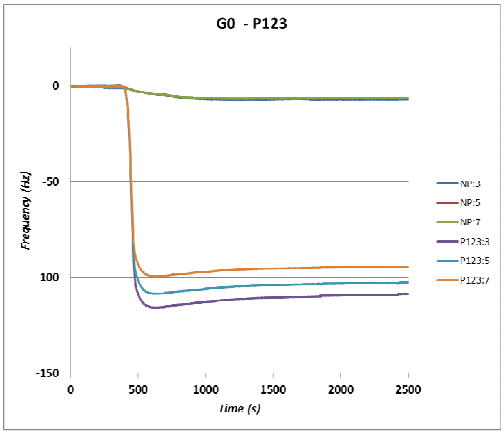

Figure 26: *QCM-D measurement presented as shifts in frequency (Δf) shows adsorption of PAMAM G0 dendrimers dissolved in methanol on non-porous and P123-derived mesoporous silica.*

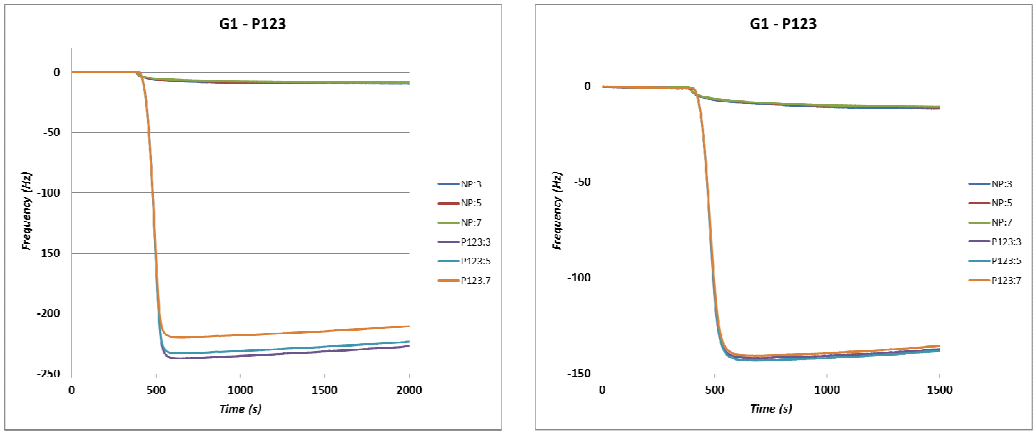

a b

Figure 27: *QCM-D measurements presented as shifts in frequency (Δf) show adsorption of PAMAM G1 dendrimers dissolved in methanol on non-porous and P123-derived mesoporous silica. (a) and (b) show the same experiment but using two different crystals prepared using different precursor solutions .*

Unfortunately, the results from the adsorption of G0 dendrimers on mesoporous silica coated crystal used in experiment 27a were not available. However, the frequency shifts for the adsorption of G0 and G1 dendrimers was the same on mesoporous silica (Fig. 26 and 27b), which clearly show that the adsorption was independent of the size of the dendrimers (1.2 and 1.8 nm, see Table 3). Since the sizes of the dendrimers were smaller than the size of the pores (5.2 nm, see Table 2) they can get access to the internal surface of the mesoporous material.

More G1 dendrimers were observed to adsorb on P123-derived mesoporous silica compare to on CTAB- or Brij S10-derived mesoporous silica. This is suggested to be related to the size of the pores of the material, which is shown to be largest for P123-derived mesoporous silica (see Table 2). Consequently, G1 dendrimers can only access the pores on P123-dervied mesoporous silica.

The adsorption of PAMAM G2 dendrimers on mesoporous and non-porous silica are presented in Figure 28. As is shown in Figure 28a, a stable frequency shift of 10 Hz was observed on non-porous silica after 70 min (4200 s). However, on mesoporous silica a stable shift in frequency was not observed after 70 min, at this point the frequency shift was measured to be 170 Hz. Unfortunately, the amount of the adsorbate solution was not enough to continue the experiment, but from the graph seems stabilize below 200 Hz.

From the results the adsorption of G0 and G1 dendrimers on mesoporous silica was observed to time independent whereas the adsorption of G2 dendrimers was observed to be time dependent. According to Table 3, G2 dendrimers have a diameter of 2.8 nm, which according to previous observations should be small enough to be able to access to the internal surfaces of the P123-derived mesopores silica (pore size, 5.2 nm).

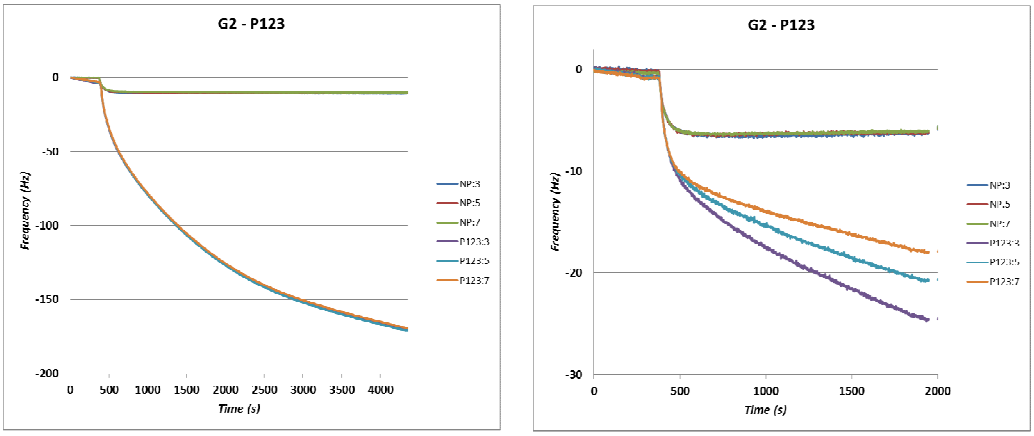

a b

Figure 28: *QCM-D measurements presented as shifts in frequency (Δf) show adsorption of PAMAM G2 dendrimers dissolved in methanol on non-porous and P123-derived mesoporous silica. (a) and (b) show the same experiment but using two different batches of crystals.*

However, G2 dendrimers are larger than G0 and G1 dendrimers (1.2 and 1.8 nm, respectively) resulting in that they needed more time to diffuse into the pores. The same results was observed for the adsorption of G0 dendrimers on CTAB-derived mesoporous silica (pore size, 2.4 nm, see Fig. 12a).

Figure 28b shows the frequency shifts obtained for the adsorption of G2 dendrimers on mesoporous silica coated crystal prepared using a different precursor solution. The obtained frequency shifts was much smaller in Figure 28b than in Figure 28a.

The smaller amount of adsorbed G2 dendrimers on mesoporous silica compare to results obtained for adsorption of G0 and G1 dendrimers is believed to be due to the size of dendrimers, as discussed previously (compare Fig. 28a with Fig. 27a and compare Fig. 28b with Fig. 27b and Fig. 26 for two different crystals).

The frequency shifts due to the adsorption of G3 dendrimers on non-porous and mesoporous silica are shown in Figure 29. The frequency shifts on non-porous silica were less than 10 Hz in all experiments. As Figure 29a shows, in one experiment the adsorption of G3 dendrimers on mesoporous silica was similar to the results obtained for the adsorption of G2 dendrimers in Figure 28a on same surfaces.

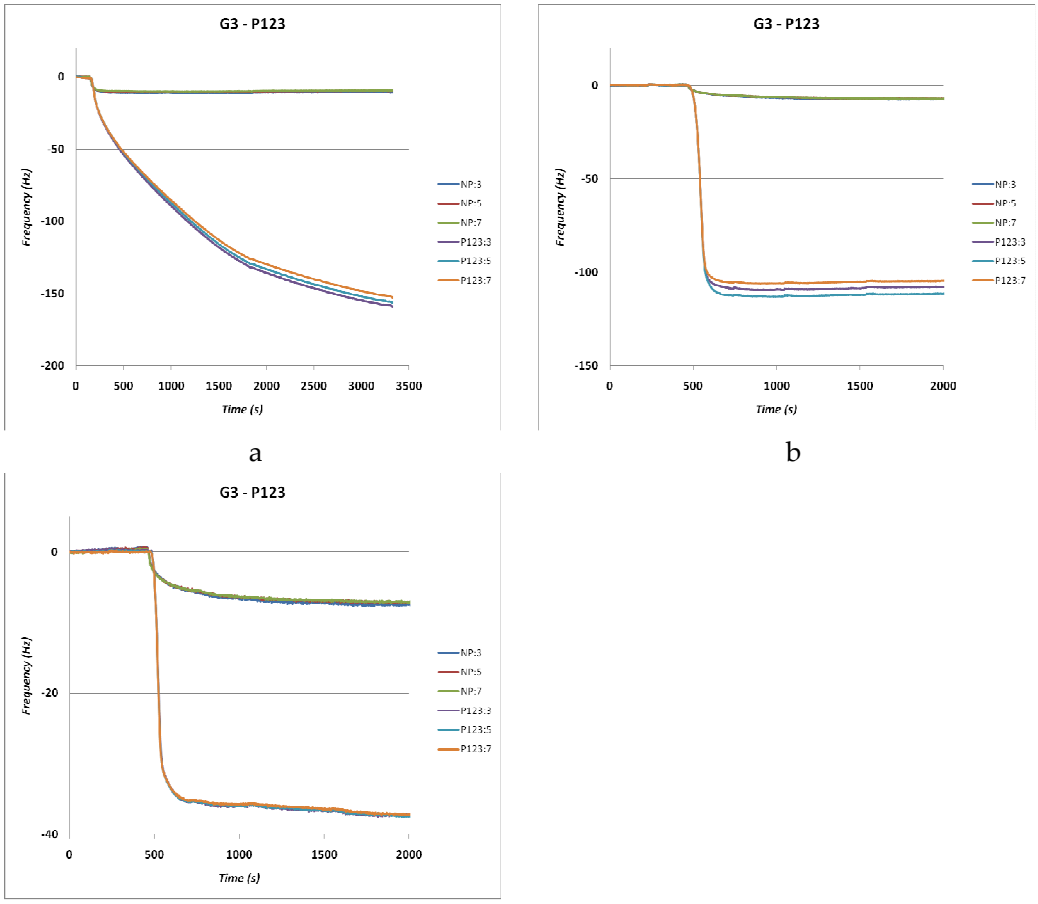

Figure 29: *QCM-D measurements presented as shifts in frequency (Δf) show adsorption of PAMAM G3 dendrimers dissolved in methanol on non-porous and P123-derived mesoporous silica. (a), (b) and (c) show the same experiment using three different batches of crystals.*

3.6.2. Adsorption of PAMAM dendrimers dispersed in water

The frequency shifts presented at three different overtones (3rd, 5th, and 7th) for the adsorption of PAMAM G0 and G3 dendrimers dispersed in water (0.1 wt.%) on non-porous (NP) and P123-derived mesoporous silica are shown in Figures 30-31.

The gradual frequency shifts on mesoporous silica upon addition of G0 dendrimers (Fig. 30a) was similar to what was observed for the adsorption of G2 and G3 dendrimers dispersed in methanol on the same crystal (see Fig. 28a and 29a). The final frequency shift around 140 Hz on mesoporous silica compared to 8-9 Hz on non-porous silica showed that dendrimers could get access to the internal surface of the pores. This indicated that the sensitivity was increased 15 times by using P123-derived mesoporous coated QCM-D compare to non-porous silica coated QCM-D crystals.

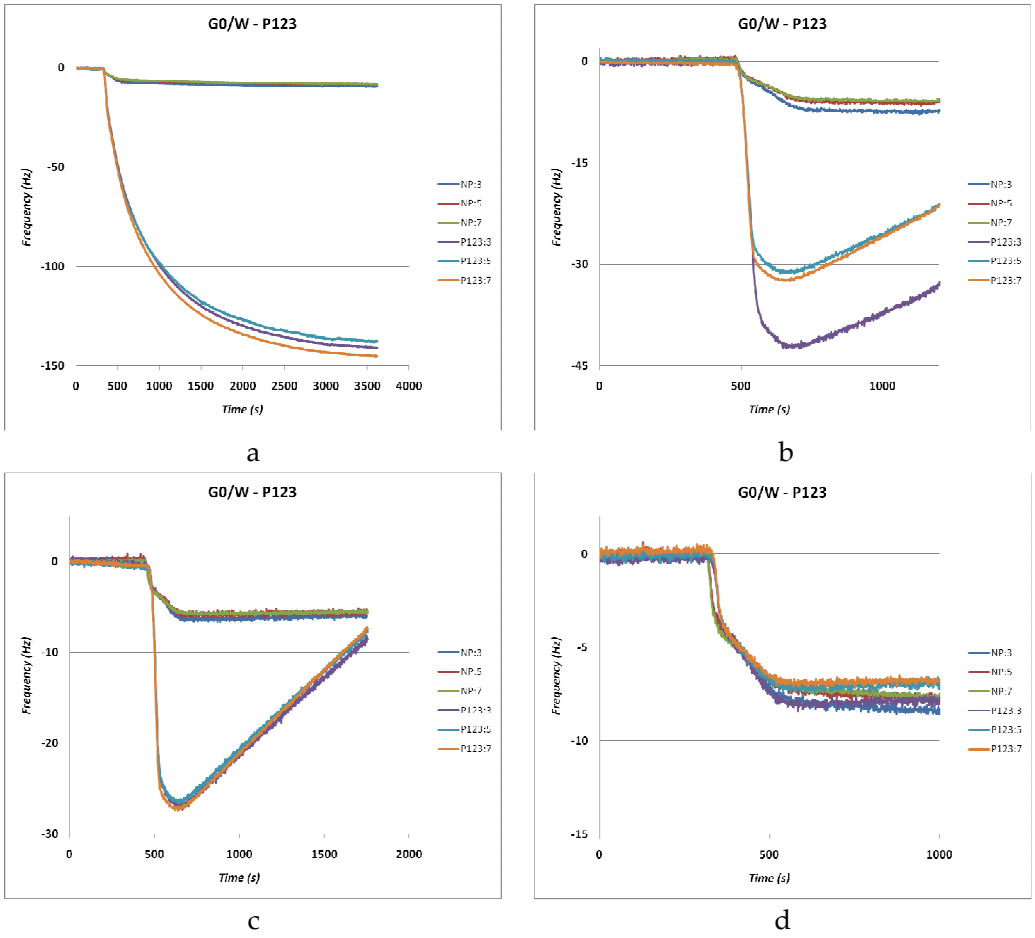

Figure 30: *QCM-D measurements presented as shifts in frequency (Δf) show adsorption of PAMAM G0 dendrimers dissolved in water on non-porous and P123-derived mesoporous silica. (a), (b) and (c) show the same experiments using two different batches of crystals and freshly prepared dendrimer solutions. (d) shows the same experiments using aged dendrimer solution.*

The adsorption of G0 dendrimers dissolved in water on P123 derived mesoporous silica (Figures 30b and 30c) was similar to results obtained for Brij S10- and CATB-derived mesoporous silica (see Fig. 16a, 16b, 23a and 23b). A rapid frequency drop (up to 27-42 Hz in different runs) was observed upon adsorption of dendrimers followed by a strong and positive drift in frequency, which may be due to the diffusion of ions through the pores.

Since the surface area of P123- and Brij S10-derived mesoporous silica were measured to be roughly the same (see Table 2) the adsorption behavior of G0 dendrimers was suggested to be similar. However, a smaller amount of G0 dendrimers was observed to be adsorbed on P123-derived mesoporous silica compared to Brij S10-derived mesoporous (see Fig. 23). This is believed to be a result of inefficiency of the cleaning procedure.

Figure 30d illustrates that the adsorption of G0 dendrimers dissolved in water one week before usage was similar on non-porous and mesoporous silica. As discussed previously, this is believed to be due to the aggregation of dendrimers in water and formation of clusters with time (see DLS measurements results, Table 3). Consequently, no difference in adsorption of G0 dendrimers was observed in terms of adsorption on non-porous and mesoporous silica.

The frequency shifts for the adsorption of G3 dendrimers dispersed in water (freshly prepared solutions and one week old solutions) on non-porous and mesoporous silica are shown in Figure 31. The adsorption of dendrimers was almost 4-8 orders of magnitude higher on mesoporous silica compared to on non-porous silica in the different runs (Fig. 31a, b and c).

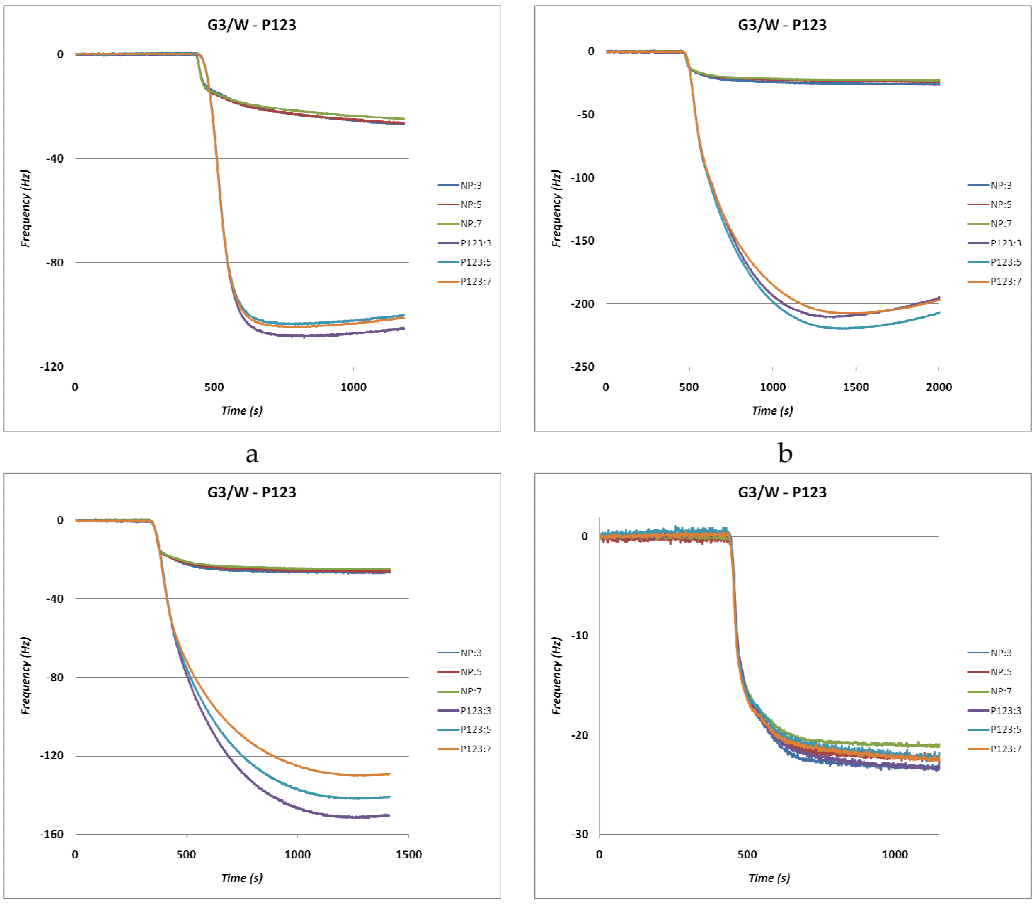

Figure 31: *QCM-D measurements presented as shifts in frequency (Δf) show adsorption of PAMAM G3 dendrimers dissolved in water on non-porous and P123-derived mesoporous silica. (a), (b) and (c) show the adsorption of freshly prepared dendrimer solution on different sets of crystals, and (d) shows the same experiments using aged dendrimer solution*

The adsorption of G3 dendrimers dissolved in water one week before analysis was similar on non-porous and mesoporous silica as is presented in Figure 31d. As mentioned previously, the observed frequency shifts for the aged solution is believed to be due to the aggregation of dendrimers in water during the aging time.

More G3 dendrimers (freshly dissolved in water) were observed to adsorb on P123-derived mesoporous silica compared to CTAB- and Brij S10-derived mesoporous silica, which could be due to its larger pore size (see Table 2).

The adsorption of G3 dendrimers dispersed in water induced higher frequency shifts on non-porous silica compared to the adsorption of G3 dendrimers dispersed in methanol. According to Figure 29 the frequency shift caused by the adsorption of G3 dendrimers dissolved in methanol were in the range of 7-10 Hz in the different experiments, whereas the frequency shifts obtained for G3 dendrimers dissolved in water were about 20-24 Hz (Fig. 31).

3.6.3. Adsorption of other substances dissolved in water

The adsorption of sodium chloride (NaCl), potassium chloride (KCl), calcium chloride ($CaCl_2$), sodium alendronate, Dimethylamine (DMA), and Tetra Ethylene Glycol (TEG) dispersed in water on non-porous and mesoporous silica were investigated using QCM-D. The results (Fig. 32) showed that the adsorption for some of these substances on P123-derived mesoporous silica differed from the results obtained on non-porous silica.

Figure 32 shows a frequency shift of 4 Hz upon the addition of TEG molecules dissolved in water on non-porous silica and 25-26 Hz on mesoporous silica. This indicated that the sensitivity was about 6 orders of magnitude larger on mesoporous silica.

The initial frequency shifts caused by the adsorption of DMA on non-porous and mesoporous silica were the same (Fig. 31b). The positive shift in frequency that was observed after the adsorption of species has been suggested to be due to "the accumulation of weakly attached particles at the liquid-crystal interface or the formation of thick viscoelastic films on the crystal surface" [45].

The observed adsorption of calcium ions on mesoporous silica was about twice as high as on non-porous silica (see Fig. 31c, the third overtone). Figure 31d shows initial frequency shift of 9 Hz on mesoporous silica compared to 1 Hz on non-porous silica upon the addition of alendronate solution. The positive drift afterward could be due to the diffusion of the ions through the mesopores.

While there was no adsorption of sodium ions on non-porous silica, a frequency shift of 6 Hz was observed for the third overtone on mesoporous silica (Fig. 31e).

The increased adsorption of these substances on P123-derived mesoporous silica compared to on CTAB- and Brij S10-derived mesoporous silica is explained by

the larger size of the pores as was obtained for P123-derived mesoporous silica (Table 2).

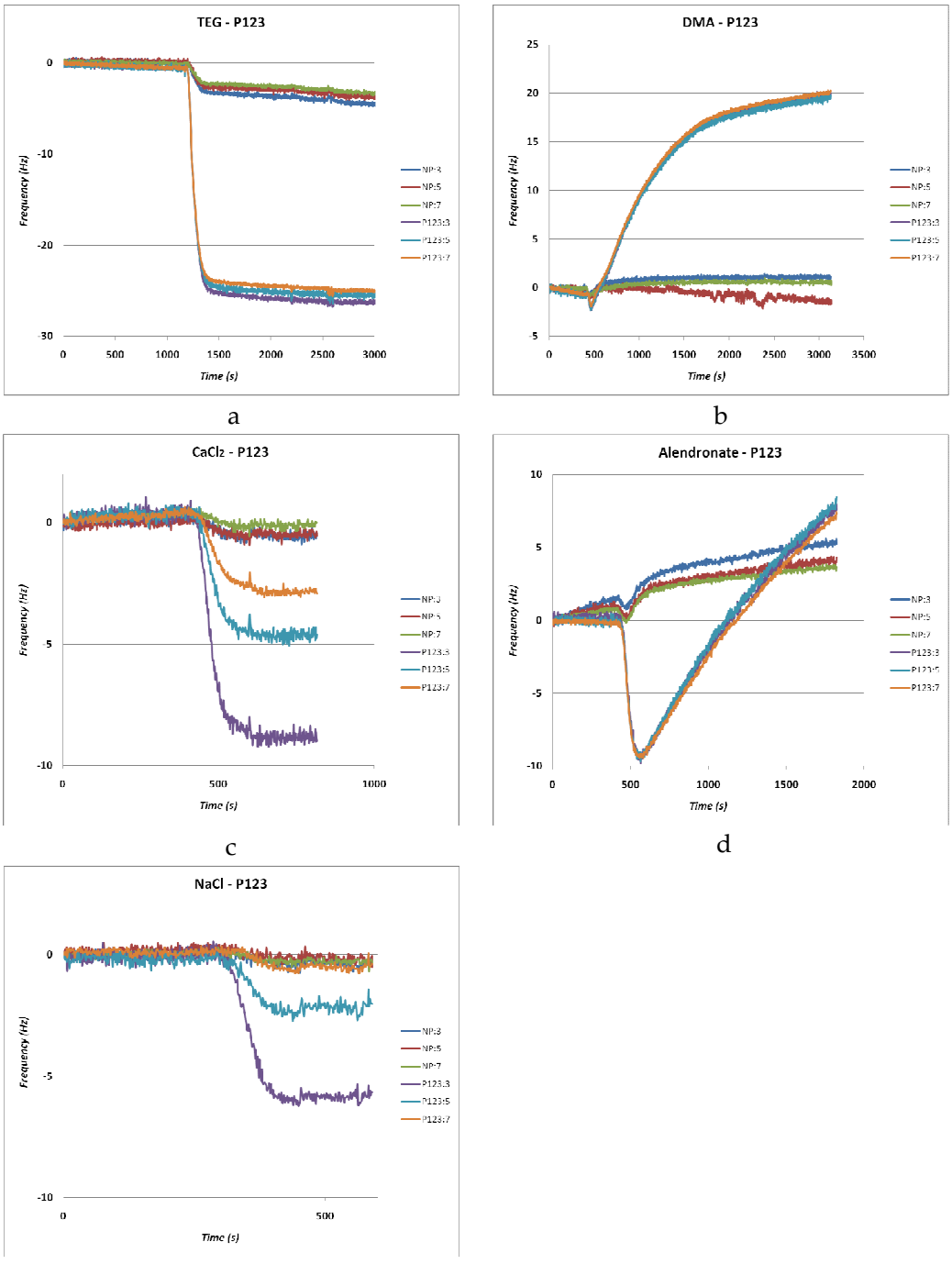

Figure 32: *QCM-D measurements presented as shifts in frequency (Δf) show adsorption of aqueous solutions of (a) Tetra Ethylene Glycol,(b) Dimethylamylamine, (c) calcium chloride, (d) sodium alendronate and (e) sodium chloride on non-porous and P123-derived mesoporous silica.*

3.7. Dissipation changes upon the adsorption of PAMAM dendrimers on mesoporous silica

Shifts in dissipation (D) were monitored during the adsorption of different PAMAM dendrimers on non-porous and mesoporous silica to study the viscoelastic properties of the adsorbed dendrimer layer on the crystal surface. For low dissipation shifts the adsorbed layer is considered to have similar properties as a rigid film, which allows the use of Sauerbrey equation (Equation 1) to calculate the mass of the adsorbed layer.

Figure 33 shows typical changes in dissipation, which were observed upon dendrimer adsorption dispersed in methanol on the various silica surfaces. The results showed that the measured changes in dissipation on non-porous silica were roughly 0.6×10^{-6} for the adsorption of G0, G1 and G2 dendrimers and 1×10^{-6} for G3 dendrimers.

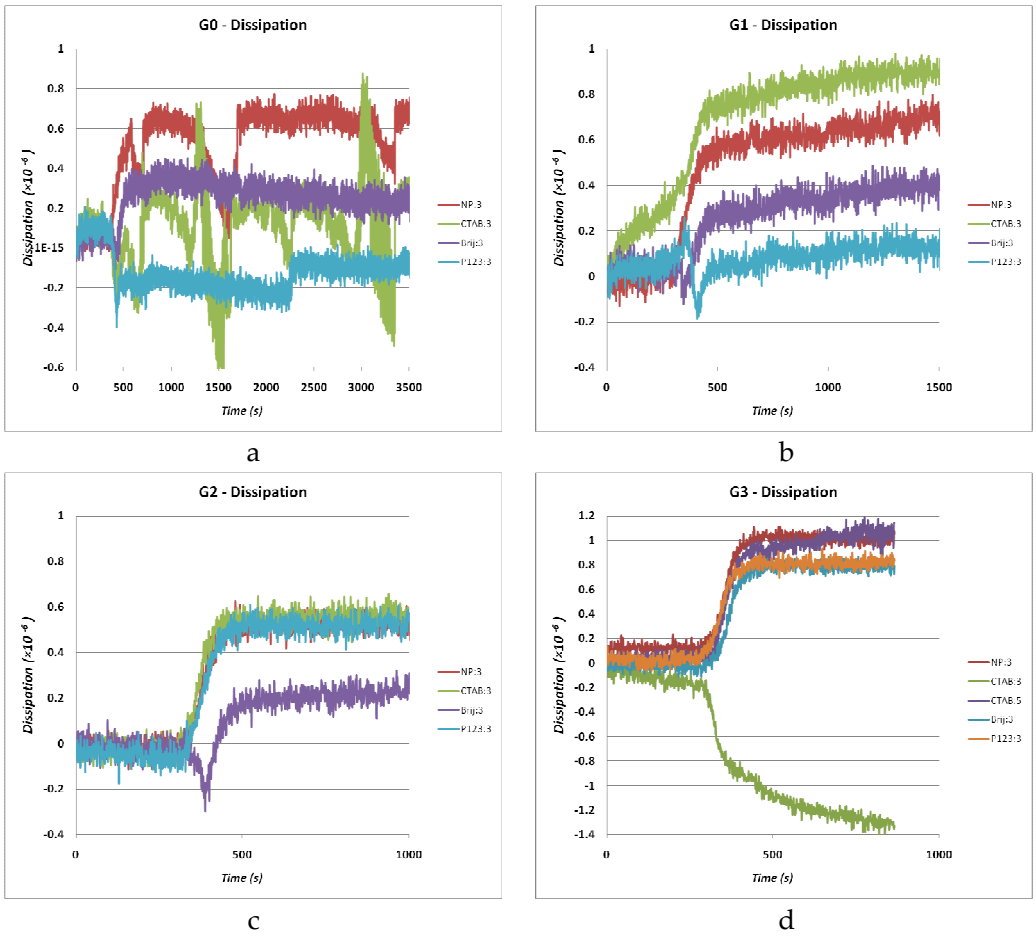

Figure 33: *Typical dissipation shifts observed during QCM-D measurements upon the adsorption of (a) G0, (b) G1, (c) G2 and (d) G3 PAMAM dendrimers dissolved in methanol on nonporous and mesoporous silica prepared using CTAB, Brij S10 and P123 as template agent.*

Similar results were obtained for the shift in dissipation on mesoporous silica. According to the results the adsorbed layers of G0, G1, G2 or G3 dendrimers were observed to be rigid on all surfaces regardless of porosity and pore size. In Figure 32d the dissipation shift for the 3rd overtone on CTAB-derived mesoporous silica was negative; however, the 5th overtone was the same as dissipation shift observed on non-porous silica.

Typical dissipation changes for the adsorption of G0 and G3 dendrimers dispersed in water are presented in Figure 33. The results showed that shifts in dissipation for the adsorption of dendrimers dispersed in water were almost twice the magnitude of the dissipation shifts obtained for the adsorption of dendrimers dissolved in methanol.

Dissipation shifts were similar on all surfaces regardless of porosity and pore size and were measured to be in the range of 1-1.5 $\times 10^{-6}$ for the adsorption of G0 dendrimers and 2-2.5$\times 10^{-6}$ for the adsorption of G3 dendrimers.

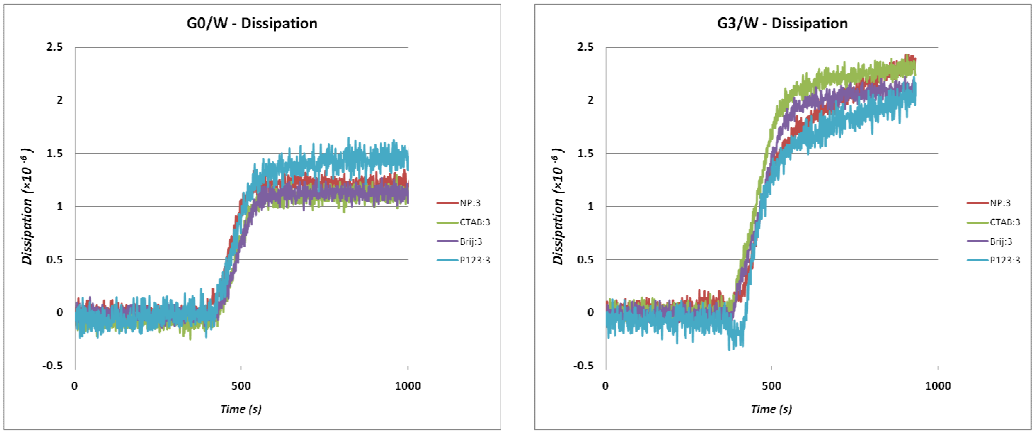

a b

Figure 33: *Typical dissipation shifts observed during QCM-D measurements upon the adsorption of (a) G0 and (b) G3 PAMAM dendrimers dissolved in water on nonporous and mesoporous silica prepared using CTAB, Brij S10 and P123 as template agent.*

4. Conclusion

The main idea behind this study was to investigate the possibility of increasing the mass sensitivity of QCM-D sensors crystals by depositing mesoporous silica thin films having varying pore sizes on the crystal surface. The advantage of using mesoporous surfaces instead of flat surfaces in sensing devises is that a larger surface area is obtained, which accordingly results in that a larger amount of adsorbate can adsorb on the surface. To investigate the possible increase in sensitivity for mesoporous material the adsorption of various adsorbates, especially PAMAM dendrimers, on non-porous and mesoporous silica has been studied using QCM-D.

The observed results revealed that mesoporous silica can improve the mass sensitivity of QCM-D crystals; however, the properties, such as pore size and surface chemistry, of the mesoporous material should be tailor-made depending on the application. The main parameters that should be considered to be adjusted are (a) the pore size of mesoporous silica relative to the adsorbate size, (b) the total accessible surface area of mesoporous silica to the adsorbates and (c) the chemical affinity of the adsorbate to silica.

For mesoporous silica having smaller pore sizes than the size of the adsorbate, the adsobates were observed to adsorb on the rough external surface. This implied an increase in mass sensitivity of the crystal of 2-5 orders of magnitude compared to non-porous silica. When the pore size of mesoporous silica was larger than the relative size of the dendrimers, the dendrimers could access to the internal surface area. This resulted in up to 30 times higher mass sensitivity of mesoporous silica than on non-porous silica.

The chemical affinity of the adsorbates to silica is another important parameter, which determines the adsorption behavior of species on mesoporous silica. Despite the strong adsorption of PAMAM dendrimers, some species showed no adsorption on the various silica surfaces. For these substances, there was no difference in adsorption on non-porous and mesoporous silica.

5. Future work

The adsorption behavior of adsorbates on mesoporous silica having larger pore sizes, than was used in this project, is suggested to be promising to study to investigate the possibility of increasing the mass sensitivity for larger molecules, such as proteins. The adsorption behavior of adsorbates on other mesoporous materials e.g. titania, can furthermore be studied to find suitable material for detecting different ions and species, which do not show affinity to silica. Finally, the adsorption behavior of adsorbents on mesoporous materials can be investigated using other techniques, such as surface Plasmon Resonance Spectroscopy (SPR) to compare the results obtained using QCM-D.

6. Acknowledgment

First of all, I would like to appreciate my supervisors Martin Andersson and Maria Claesson for their constant support and advices. Martin introduced me this interesting field of science and gave me the opportunity to work in his group and Maria helped me to do the project step by step, from the first day of my diploma work to the final writing steps.

I am sincerely grateful to Prof. Krister Holmberg for giving me the permission to work in the division of Applied Surface Chemistry and examining the work.

I also would like to thank all the people at TYK for providing me the friendly working atmosphere and specially Martin's group members for nice group meetings.

Many thanks to my roommates and friends in the master student's room for providing such a pleasant environment during my work in this department.

Most importantly, I would like to show my sincere gratitude to my lovely family, especially my mother, for their patience with all my flaws and their support in all my life.

Finally, I wish to express my deep thanks to Hedieh, my beloved wife who has suffered so much from my work, for her love, her understanding, and her great support and encouragement.

7. References

1. Adhikari, B. and S. Majumdar, *Polymers in sensor applications.* Prog. Polym. Sci. , 2004. 29(7): p. 699-766.
2. Gast, T., et al., *Survey on mass determination systems - Part I. Fundamentals and history.* Journal of Thermal Analysis and Calorimetry, 2003. 71(1): p. 19-23.
3. Sauerbrey, G., *Verwendung Von Schwingquarzen Zur Wagung Dunner Schichten Und Zur Mikrowagung.* Zeitschrift Fur Physik, 1959. 155(2): p. 206-222.
4. Janata, J.r., *Principles of chemical sensors*. 2nd ed2009, Dordrecht ; New York: Springer. xv, 373 p.
5. Andersson, M., et al., *Quartz crystal microbalance-with dissipation monitoring (QCM-D) for real time measurements of blood coagulation density and immune complement activation on artificial surfaces.* Biosens. Bioelectron., 2005. 21(1): p. 79-86.
6. Arnau, A., *A review of interface electronic systems for AT-cut quartz crystal microbalance applications in liquids.* Sensors, 2008. 8(1): p. 370-411.
7. Dixon, M.C., *Quartz crystal microbalance with dissipation monitoring: enabling real-time characterization of biological materials and their interactions.* J Biomol Tech, 2008. 19(3): p. 151-8.
8. Steinem, C., et al., *The QCM-D Technique for Probing Biomacromolecular Recognition Reactions*, in *Piezoelectric Sensors*, O.S. Wolfbeis, Editor 2007, Springer Berlin Heidelberg. p. 425-447.
9. Nomura, T. and M. Okuhara, *Frequency-Shifts of Piezoelectric Quartz Crystals Immersed in Organic Liquids.* Anal. Chim. Acta 1982. 142(Oct): p. 281-284.
10. Rodahl, M., et al., *Quartz-Crystal Microbalance Setup for Frequency and Q-Factor Measurements in Gaseous and Liquid Environments.* Rev. Sci. Instrum. , 1995. 66(7): p. 3924-3930.
11. Marx, K.A., *Quartz crystal microbalance: A useful tool for studying thin polymer films and complex biomolecular systems at the solution-surface interface.* Biomacromolecules, 2003. 4(5): p. 1099-1120.
12. Höök F., R.M., *Quartz crystal microbalances (QCM) in biomacromolecular recognition.* 2005.
13. Burwell, R.L., *Manual of Symbols and Terminology for Physicochemical Quantities and Units - Appendix 2 - Definitions, Terminology and Symbols in Colloid and Surface-Chemistry .2. Heterogeneous Catalysis.* Pure Appl. Chem., 1976. 46(1): p. 71-&.
14. Corma, A., *From microporous to mesoporous molecular sieve materials and their use in catalysis.* Chem. Rev., 1997. 97(6): p. 2373-2419.
15. Yanagisawa, T., et al., *The Preparation of Alkyltrimethylammonium-Kanemite Complexes and Their Conversion to Microporous Materials.* Bull. Chem. Soc. Jpn., 1990. 63(4): p. 988-992.
16. Kresge, C.T., et al., *Ordered Mesoporous Molecular-Sieves Synthesized by a Liquid-Crystal Template Mechanism.* Nature, 1992. 359(6397): p. 710-712.

17. Beck, J.S., et al., *A New Family of Mesoporous Molecular-Sieves Prepared with Liquid-Crystal Templates.* J. Am. Chem. Soc., 1992. 114(27): p. 10834-10843.
18. CHIOLA VINCENT, R.J.E., VANDERPOOL CLARENCE D, *Process for producing low-bulk density silica* US Patent, 1971. (No. 3556725).
19. DiRenzo, F., *A 28-year-old synthesis of micelle-templated mesoporous silica.* Microporous Materials, 1997. 10(4-6): p. 283-286.
20. James C. Vartuli, W.J.R., Thomas F. Degnan, Jr., *Mesoporous Materials (M41S): From Discovery to Application*, in *Dekker Encyclopedia of Nanoscience and Nanotechnology* C.I.C. James A. Schwarz, Karol Putyera, Editor 2004, CRC Press p. Chapter 114.
21. Norhasyimi Rahmat, A.Z.A., Abdullah R. Mohamed, *A Review: Mesoporous Santa Barbara Amorphous-15, Types, Synthesis and Its Applications towards Biorefinery Production.* American Journal of Applied Sciences, 2010. 7(12): p. 1579-1586.
22. Brinker, C.J., et al., *Evaporation-induced self-assembly: Nanostructures made easy.* Adv. Mater., 1999. 11(7): p. 579-585.
23. Oye, G., J. Sjoblom, and M. Stocker, *Synthesis, characterization and potential applications of new materials in the mesoporous range.* Adv. Colloid Interface Sci., 2001. 89: p. 439-466.
24. Raman, N.K., M.T. Anderson, and C.J. Brinker, *Template-based approaches to the preparation of amorphous, nanoporous silicas.* Chem. Mat., 1996. 8(8): p. 1682-1701.
25. Tomalia, D.A., et al., *Dendrimers as reactive modules for the synthesis of new structure-controlled, higher-complexity megamers.* Pure and Applied Chemistry, 2000. 72(12): p. 2343-2358.
26. Tomalia, D.A. and J.M.J. Frechet, *Discovery of dendrimers and dendritic polymers: A brief historical perspective.* J. Polym. Sci. Pol. Chem., 2002. 40(16): p. 2719-2728.
27. Tomalia, D.A., et al., *Dendritic Macromolecules - Synthesis of Starburst Dendrimers.* Macromolecules, 1986. 19(9): p. 2466-2468.
28. Ottaviani, M.F., et al., *EPR investigation of the adsorption of dendrimers on porous surfaces.* J. Phys. Chem. B, 2003. 107(9): p. 2046-2053.
29. McCain, K.S., P. Schluesche, and J.M. Harris, *Modifying the adsorption behavior of polyamidoamine dendrimers at silica surfaces investigated by total internal reflection fluorescence correlation spectroscopy.* Anal. Chem., 2004. 76(4): p. 930-938.
30. Holister, P.C.R.V., Tim Harper *Dendrimers: Technology White Papers*, 2003, Cientifica, Ltd.
31. Esfand, R. and D.A. Tomalia, *Poly(amidoamine) (PAMAM) dendrimers: from biomimicry to drug delivery and biomedical applications.* Drug Discov. Today, 2001. 6(8): p. 427-436.
32. Pisal, D.S., et al., *Permeability of surface-modified polyamidoamine (PAMAM) dendrimers across Caco-2 cell monolayers.* Int. J. Pharm., 2008. 350(1-2): p. 113-121.

33. Besson, S., et al., *Phase diagram for mesoporous CTAB-silica films prepared under dynamic conditions.* J. Mater. Chem., 2003. 13(2): p. 404-409.
34. Jung, S.B. and H.H. Park, *Concentration-dependent mesostructure of surfactant-templated mesoporous silica thin film.* Thin Solid Films, 2006. 494(1-2): p. 320-324.
35. Alberius, P.C.A., et al., *General predictive syntheses of cubic, hexagonal, and lamellar silica and titania mesostructured thin films.* Chem. Mat., 2002. 14(8): p. 3284-3294.
36. Groen, J.C., L.A.A. Peffer, and J. Perez-Ramirez, *Pore size determination in modified micro- and mesoporous materials. Pitfalls and limitations in gas adsorption data analysis.* Microporous Mesoporous Mat., 2003. 60(1-3): p. 1-17.
37. Sing, K.S.W., et al., *Reporting Physisorption Data for Gas Solid Systems with Special Reference to the Determination of Surface-Area and Porosity (Recommendations 1984).* Pure Appl. Chem., 1985. 57(4): p. 603-619.
38. Williams, D.B. and C.B. Carter, *Transmission electron microscopy : a textbook for materials science*1996, New York: Plenum Press. xxvii, 729 p.
39. *Dynamic Light Scattering: An Introduction in 30 Minutes*, Malvern Instruments Ltd
40. Halford, B., *Dendrimers branch out.* Chem. Eng. News, 2005. 83(24): p. 30-36.
41. *PAMAM Dendrimers* 2011,04,20]; Available from: http://www.dendritech.com/pamam.html.
42. Zhang, X.E., et al., *Direct synthesis and characterization of highly ordered functional mesoporous silica thin films with high amino-groups content.* Appl. Surf. Sci., 2008. 254(9): p. 2893-2899.
43. Thommes, M., R. Kohn, and M. Froba, *Sorption and pore condensation behavior of nitrogen, argon, and krypton in mesoporous: MCM-48 silica materials.* J. Phys. Chem. B, 2000. 104(33): p. 7932-7943.
44. Esumi, K. and M. Goino, *Adsorption of poly(amidoamine) dendrimers on aluminan-water and silica/water interfaces.* Langmuir, 1998. 14(16): p. 4466-4470.